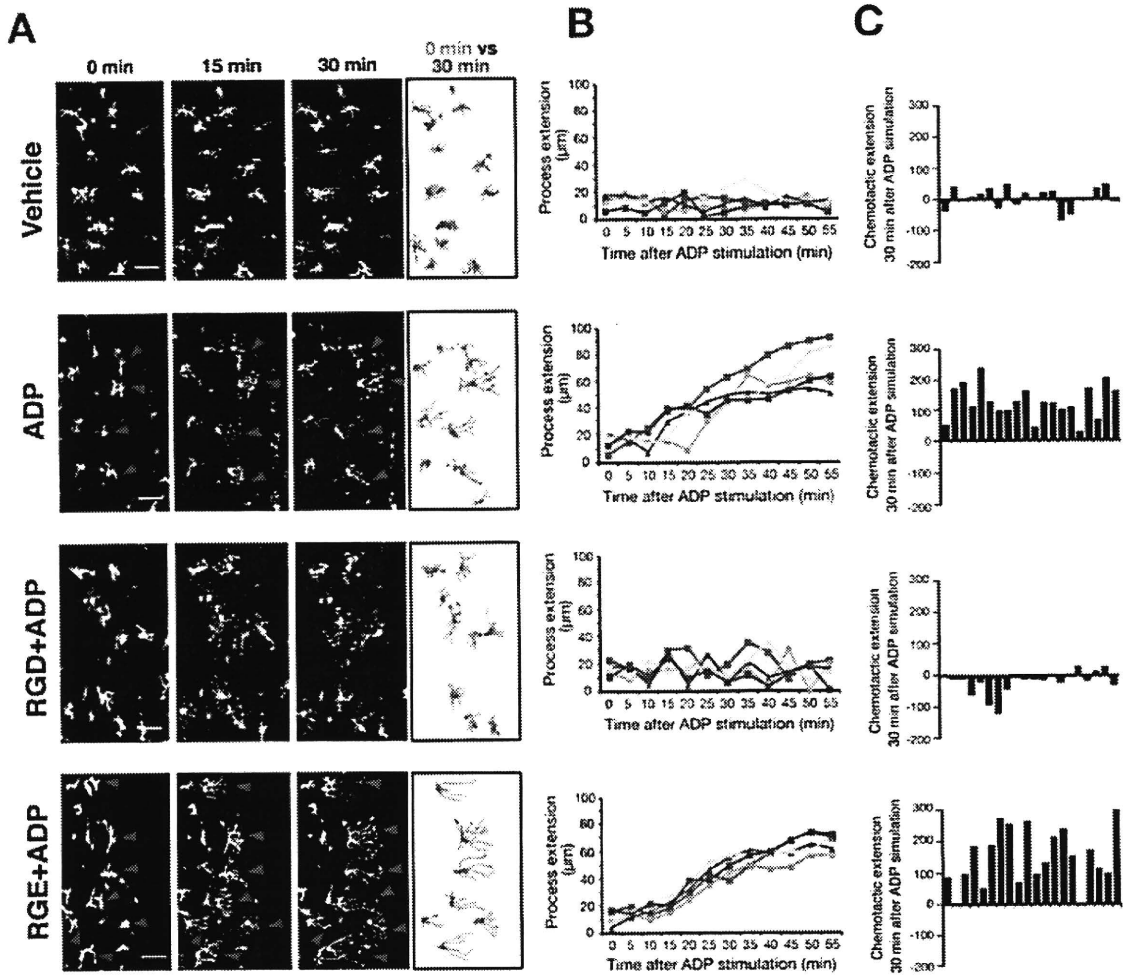

Fig. 7. RGD peptides inhibit the process extension by microglia responding to exogenous nucleotides in brain slices. (A) Microglia in hippocampal slices from neonatal (p4-7) EGFP-expressing mice were examined by time-lapse confocal imagng. Microglia extended long processes (red arrowheads) toward the periphery of the slices (right side of each frame) at various time points following addition of 1 mM ADP to the bath. In the presence of 1 mM RGE peptides microglia extended processes toward the periphery of the slices, whereas no long process extension toward the periphery of the slices was observed in the presence of 1 mM RGD peptides. Morphology of microglia at time 0 (green) and 30 min later (red) is depicted in the panel on the far right. (B) Microglial process length (μm) in slices measured at each time point indicated (five processes per cell). Positive length change indicates extension, whereas negative length change indicates retraction. RGE-treated microglia continuously extended their processes, whereas RGD-treated microglia repeatedly extended and retracted their processes. (C) Chemotaxis of the process extension responding to ADP addition in the absence and presence of RGD and RGE peptides. The degree of chemotactic extension (μm) of each cell is expressed by the difference obtained by subtracting the total length of the branches extending away from the nucleotide source from the total length of branches extending toward the periphery of the slices. Twenty cells residing in the stratum pyramidale and stratum oriens of the CA3 area of the hippocampus were examined 30 min after the addition of ADP. In the presence of RGE peptides, microglia extended their processes toward the ADP source the same as when stimulated with ADP alone, whereas directional process extension decreased in the presence of RGD peptides.

hippocampal slices prepared from neonatal (p4-7) Iba1-EGFP transgenic mice (Hirasawa et al., 2005), whose microglia are easily detected by EGFP signals. To analyze the initial response of microglia to ADP, we monitored the behavior of microglia expressing EGFP by time-lapse microphotography for 1 h following exposure to 1 mM ADP in the bath. The microglia in unstimulated slices repeatedly extended and retracted processes a short distance, but their cell bodies did not migrate. When slices were exposed to ADP, most of the microglia did not migrate from their original position for a period of 1 h and they rapidly extended their long processes toward the periphery of the slices within 5 min, and the extension was sustained for 1 h (Fig. 7A, Supp. Info. Video 1). We confirmed that the process extension in the ADP-stimulated slices was suppressed by treating the slices with AR-C69931MX (10 μM), indicating that $P2Y_{12}$ mediated the process extension by microglia in the culture slices (data not shown). Pretreating slices with RGD peptides (1 mM) significantly inhibited the rapid process extension by microglia toward the periphery of the slices, whereas pretreating slices with RGE peptides (1 mM) had no effect on the process extension by microglia (Fig. 7C,D, Supp. Info. Video 2). Following ADP exposure, the microglia in the RGD-pretreated slices sent out many processes in random directions, and

the processes were often extended to nearly 40 μm but immediately retracted. These findings indicate that blocking of the integrin-ECM interaction with RGD peptides suppressed directional process extension by microglia in brain tissue.

DISCUSSION

In this study, we used collagen gel to establish an *in vitro* assay system to analyze the molecular mechanisms that regulate process extension by microglia. Morphological changes and migration by microglia have previously been studied by using two-dimensional culture systems, such as the Boyden chamber (Nolte et al., 1997) or the Dunn chemotaxis chamber (Honda et al., 2001; Webb et al., 1996). However, it has not been possible to reproduce the directional process extension by microglia observed in brain tissues with these systems. The cell culture system using 3D matrices is known as a model that mimics the state of cells in tissue and has been reported to be useful for examination of cell motility and signaling events (Cukierman et al., 2002). We therefore plated microglia on 3D-collagen gels in the insert of a transwell chamber, and we were able to show that the cells extended their processes into the gels in an ATP-gradient-dependent manner.

Our findings strongly suggest that an integrin-β1-ECM interaction is involved in the directional process extension. Microglial adhesion to collagen gel was weak under unstimulated conditions, and ATP increased the strength of the microglial adhesion to the gel. The RGD peptides and the functional blocking antibody against integrin-β1 inhibited the cell adhesion and the process extension into the gels, and the RGD peptides significantly inhibited ADP-induced process extension by microglia in hippocampal slices. ECM molecules that bind to integrin-β1, such as fibronectin, vitronectin, and laminin, have been reported to be slightly expressed in the normal brain and localize in microblood vessels (Bellail et al., 2004; Krum et al., 1991). Previous studies have shown that microglia attach weakly to laminin and ECM of astrocytes, and that laminin exerts a dominant anti-adhesive effect on microglial adhesion to astrocytes (Milner and Campbell, 2002b). Accordingly, most of the integrin-β1 in microglia in the normal brain seems to be inactivated. Collagen type-I is considered to be an artificial substrate for microglia because neither collagen fibers nor collagen-rich basal laminas are present in the CNS (Jones, 1996). However, the weak adhesion by microglia to collagen gels suggest that the microglia cultured in the gels maintain integrin-β1 in an inactivated state, the same as microglia in brain tissue. Accumulating studies have demonstrated that laminins are expressed by astrocytes and neurons in the adult brain and are involved in axon growth and guidance (Grimpe et al., 2002; Jucker et al., 1991; Liesi, 1990; Zhou, 1990). We confirmed that microglia attach weakly to laminin-coated dishes and that ATP induces an increase in microglial adhesion to laminin (data not shown). These observations suggest that laminins are candidates for the molecules that bind integrin-β1 to achieve the ATP/ADP-induced process extension by microglia in brain tissue.

In the normal brain, microglia express integrin-β2, LFA1 (αLβ2), and CD11b/CD18 (αMβ2) (Kloss et al., 1999). Previous studies have shown that the rapid change in microglial morphology and migration by microglia toward injured neurons in hippocampal slices are unaffected in tissue slices from integrin-β2 deficient mice (Kurpius et al., 2006). Although these studies suggest that integrin-β2 is not involved in the early activation of microglial motility, we were unable to completely rule out a role of integrin-β2 in process extension. Further study will be necessary to identify the subtypes of integrins that are involved in the rapid process extension in brain tissue.

The increase in cell adhesion requires that integrins become "activated" by undergoing conformational changes regulated by inside-out signals (Hynes, 2002; Kinashi, 2005). ATP/ADP increased the microglial adhesion to collagen gels, and the increase was inhibited by RGD peptides, a functional blocking antibody against integrin-β1, and a $P2Y_{12}$ selective antagonist, AR-C69931MX. ATP increased the active integrin-β1 level in $P2Y_{12}$-expressing 1321N1 cells but not in wild-type cells. These results demonstrate that $P2Y_{12}$ mediates the ATP-induced activation of integrin-β1. Stimulation of G protein-coupled receptors activates several signaling pathways, including the PI3K, PLC, RAS, and Rho family small GTPase, and mitogen-activated protein kinase (MAPK) signaling cascades, some of which have been implicated in the inside-out signaling (Hynes, 2002; Kinashi, 2005). In this study, we showed that activation of both PI3K and PLC signaling pathways downstream of $P2Y_{12}$ is required for the ATP-induced process extension by microglia. In addition, we examined the effect of PI3K and PLC inhibitors on the ATP-induced increase in microglial adhesion to collagen gels. Pretreatment with the PLC inhibitor U73122 (100 nM) inhibited cell adhesion, whereas the PI3K inhibitor LY294002 (50 μM) had no effect (data not shown), suggesting that PLC activation is required for activation of integrin-β1 but that PI3K activation is not. Previous studies have demonstrated that binding of the cytoplasmic actin-bindng protein talin to the β integrins tail is crucial for the activation of β integrins (Tadokoro et al., 2003), and the small GTPase Rap1 has been reported to regulate talin binding to β integrins through C-kinase and calcium signaling pathways downstream of PLC (Franke et al., 1997, 2000; Han et al., 2006). Thus, Rap1-Talin cascades may be involved in $P2Y_{12}$-mediated activation of integrin-β1 in microglia. However, further works are needed to determine which of the aforementioned regulatory mechanisms is relevant in microglia.

As described in previous reports (Haynes et al., 2006; Kurpius et al., 2007), time-lapse imaging of EGFP-labeled microglia in hippocampal slices showed that addition of ADP to the bath immediately induced process extension by microglia toward periphery of the slices.

Immunohistochemical staining revealed that integrin-β1 had accumulated in the tips of the microglial projections extending toward the periphery of the slices following ADP application. The microglia in slices pretreated with RGD peptides sent out many projections in random directions within 10 min following exposure to ADP, but the microglia retracted the projections and did not continue extending them toward the ADP sources. These observations strongly suggest that interaction between integrin-β1 and the ECM is necessary for microglia to direct their processes and to maintain the elongated processes. Binding of integrin-β1 to ligands is known to promote integrin clustering, activate outside-in signaling pathways, and lead to actin-cytoskeleton reorganization (Berrier and Yamada, 2007). The dot-like staining of integrin-β1 in the tips of microglial processes, as shown in Fig. 6, suggests that the clustered integrin-β1 activates integrin signaling pathways. Activation of the signaling pathways downstream of integrin-β1 may act as positive feedback signals and cooperate with the signaling pathways downstream of $P2Y_{12}$ to regulate directional process extension by microglia.

Most of the microglia on the collagen gel in the process extension assay did not migrate toward ATP within 2 h after ATP stimulation. However, we observed that microglia had migrated into collagen gels toward the ATP after incubation for 4h, and that RGD peptide inhibited the cell migration (data not shown). These observations suggest that integrin-β1 activation is involved in the movement of micoglial cell bodies and that the cell migration requires activation of other signaling pathways in addition to those underlying the process extension. Integrin-β has been reported to be upregulated by activated microglia in pathological states, such as nerve injury or ischemia, (Kang et al., 2008; Kloss et al., 1999). Expression of ECM ligands for integrin-β1 is increased in pathological states, and fibronectin leak to brain parenchyma from blood vessels when blood-brain-barrier is damaged by some pathological conditions (Liesi et al., 1984; Nasu-Tada et al., 2006; Tate et al., 2007). Interactions between integrins and fibronectin have been reported to regulate microglial migration, proliferation, and protein expression (Milner et al., 2007; Nasu-Tada et al., 2005, 2006). The ECM binding to integrins activates intracellular signalings that regulate microglial motility, and therefore may be an important signal for regulating the extent of microglial infiltration at the site of injury and retention there.

In this study, we demonstrated immunohistochemically that the microglia in normal brains express integrin-β1. Most of the integrin-β1 in microglia in the normal brain seems to be inactivated because ECM molecules that bind to integrin-β1 have been reported to be slightly expressed in the normal brain. (Bellail et al., 2004). In the early stage following neuronal injury, ATP may induce integrin-β1 activation in microglia through $P2Y_{12}$. The integrin-β1 activation increases microglial adhesion to the ECM, and that may be an important trigger for process extension by microglia toward the injured region. $P2Y_{12}$-dependent integrin-β1 activation may be crucial for inducing the initial response of microglia to brain damage.

ACKNOWLEDGMENTS

We thank Drs. S. Uchino and T. Namba for advice and discussion.

REFERENCES

Bellail AC, Hunter SB, Brat DJ, Tan C, Van Meir EG. 2004. Microregional extracellular matrix heterogeneity in brain modulates glioma cell invasion. Int J Biochem Cell Biol 36:1046–1069.

Berrier AL, Yamada KM. 2007. Cell-matrix adhesion. J Cell Physiol 213:565–573.

Bo L, Peterson JW, Mork S, Hoffman PA, Gallatin WM, Ranschoff RM, Trapp BD. 1996. Distribution of immunoglobulin superfamily members ICAM-1, -2, -3, and the beta 2 integrin LFA-1 in multiple sclerosis lesions. J Neuropathol Exp Neurol 55:1060–1072.

Burnstock G. 2008. Purinergic signalling and disorders of the central nervous system. Nat Rev Drug Discov 7:575–590.

Cukierman E, Pankov R, Yamada KM. 2002. Cell interactions with three-dimensional matrices. Curr Opin Cell Biol 14:633–639.

Davalos D, Grutzendler J, Yang G, Kim JV, Zuo Y, Jung S, Littman DR, Dustin ML, Gan WB. 2005. ATP mediates rapid microglial response to local brain injury in vivo. Nat Neurosci 8:752–758.

Filtz TM, Li Q, Boyer JL, Nicholas RA, Harden TK. 1994. Expression of a cloned P2Y purinergic receptor that couples to phospholipase C. Mol Pharmacol 46:8–14.

Franke B, Akkerman JW, Bos JL. 1997. Rapid Ca2+-mediated activation of Rap1 in human platelets. EMBO J 16:252–259.

Franke B, van Triest M, de Bruijn KM, van Willigen G, Nieuwenhuis HK, Negrier C, Akkerman JW, Bos JL. 2000. Sequential regulation of the small GTPase Rap1 in human platelets. Mol Cell Biol 20:779–785.

Franke H, Krugel U, Illes P. 2006. P2 receptors and neuronal injury. Pflugers Arch 452:622–644.

Grimpe B, Dong S, Doller C, Temple K, Malouf AT, Silver J. 2002. The critical role of basement membrane-independent laminin gamma 1 chain during axon regeneration in the CNS. J Neurosci 22:3144–3160.

Han J, Lim CJ, Watanabe N, Soriani A, Ratnikov B, Calderwood DA, Puzon-McLaughlin W, Lafuente EM, Boussiotis VA, Shattil SJ, Ginsberg MH. 2006. Reconstructing and deconstructing agonist-induced activation of integrin alphaIIbbeta3. Curr Biol 16:1796–1806.

Haynes SE, Hollopeter G, Yang G, Kurpius D, Dailey ME, Gan WB, Julius D. 2006. The $P2Y_{12}$ receptor regulates microglial activation by extracellular nucleotides. Nat Neurosci 9:1512–1519.

Hirasawa T, Ohsawa K, Imai Y, Ondo Y, Akazawa C, Uchino S, Kohsaka S. 2005. Visualization of microglia in living tissues using Iba1-EGFP transgenic mice. J Neurosci Res 81:357–362.

Honda S, Sasaki Y, Ohsawa K, Imai Y, Nakamura Y, Inoue K, Kohsaka S. 2001. Extracellular ATP or ADP induce chemotaxis of cultured microglia through Gi/o-coupled P2Y receptors. J Neurosci 21:1975–1982.

Hynes RO. 2002. Integrins: Bidirectional, allosteric signaling machines. Cell 110:673–687.

Imai Y, Ibata I, Ito D, Ohsawa K, Kohsaka S. 1996. A novel gene iba1 in the major histocompatibility complex class III region encoding an EF hand protein expressed in a monocytic lineage. Biochem Biophys Res Commun 224:855–862.

Inoue K. 2006. The function of microglia through purinergic receptors: Neuropathic pain and cytokine release. Pharmacol Ther 109:210–226.

Irino Y, Nakamura Y, Inoue K, Kohsaka S, Ohsawa K. 2008. Akt activation is involved in $P2Y_{12}$ receptor-mediated chemotaxis of microglia. J Neurosci Res 86:1511–1519.

Jones LS. 1996. Integrins: Possible functions in the adult CNS. Trends Neurosci 19:68–72.

Jucker M, Kleinman HK, Hohmann CF, Ordy JM, Ingram DK. 1991. Distinct immunoreactivity to 110 kDa laminin-binding protein in adult and lesioned rat forebrain. Brain Res 555:305–312.

Kang WS, Choi JS, Shin YJ, Kim HY, Cha JH, Lee JY, Chun MH, Lee MY. 2008. Differential regulation of osteopontin receptors, CD44 and the alpha(v) and beta(3) integrin subunits, in the rat hippocampus following transient forebrain ischemia. Brain Res 1228:208–216.

Kinashi T. 2005. Intracellular signalling controlling integrin activation in lymphocytes. Nat Rev Immunol 5:546–559.

Kloss CU, Werner A, Klein MA, Shen J, Menuz K, Probst JC, Kreutzberg GW, Raivich G. 1999. Integrin family of cell adhesion molecules in the injured brain: Regulation and cellular localization in the normal and regenerating mouse facial motor nucleus. J Comp Neurol 411:162–178.

Koizumi S, Fujishita K, Tsuda M, Shigemoto-Mogami Y, Inoue K. 2003. Dynamic inhibition of excitatory synaptic transmission by astrocyte-derived ATP in hippocampal cultures. Proc Natl Acad Sci USA 100:11023–11028.

Kreutzberg GW. 1996. Microglia: A sensor for pathological events in the CNS. Trends Neurosci 19:312–318.

Krum JM, More NS, Rosenstein JM. 1991. Brain angiogenesis: Variations in vascular basement membrane glycoprotein immunoreactivity. Exp Neurol 111:152–165.

Kurpius D, Nolley EP, Dailey ME. 2007. Purines induce directed migration and rapid homing of microglia to injured pyramidal neurons in developing hippocampus. Glia 55:873–884.

Kurpius D, Wilson N, Fuller L, Hoffman A, Dailey ME. 2006. Early activation, motility, and homing of neonatal microglia to injured neurons does not require protein synthesis. Glia 54:58–70.

Liesi P. 1990. Extracellular matrix and neuronal movement. Experientia 46:900–907.

Liesi P, Kaakkola S, Dahl D, Vaheri A. 1984. Laminin is induced in astrocytes of adult brain by injury. EMBO J 3:683–686.

Milner R, Campbell IL. 2002a. The integrin family of cell adhesion molecules has multiple functions within the CNS. J Neurosci Res 69:286–291.

Milner R, Campbell IL. 2002b. Cytokines regulate microglial adhesion to laminin and astrocyte extracellular matrix via protein kinase C-dependent activation of the alpha6beta1 integrin. J Neurosci 22:1562–1572.

Milner R, Crocker SJ, Hung S, Wang X, Frausto RF, del Zoppo GJ. 2007. Fibronectin- and vitronectin-induced microglial activation and matrix metalloproteinase-9 expression is mediated by integrins alpha5beta1 and alphavbeta5. J Immunol 178:8158–8167.

Nakajima K, Kohsaka S. 2005. Response of microglia to brain injury. In: Kettenmann H, Ransom B, editors. Neuroglia, 2nd ed. New York: Oxford University Press. pp 443–453.

Nakajima K, Shimojo M, Hamanoue M, Ishiura S, Sugita H, Kohsaka S. 1992. Identification of elastase as a secretory protease from cultured rat microglia. J Neurochem 58:1401–1408.

Nasu-Tada K, Koizumi S, Inoue K. 2005. Involvement of beta1 integrin in microglial chemotaxis and proliferation on fibronectin: Different regulations by ADP through PKA. Glia 52:98–107.

Nasu-Tada K, Koizumi S, Tsuda M, Kunifusa E, Inoue K. 2006. Possible involvement of increase in spinal fibronectin following peripheral nerve injury in upregulation of microglial $P2X_4$, a key molecule for mechanical allodynia. Glia 53:769–775.

Neumann J, Sauerzweig S, Ronicke R, Gunzer F, Dinkel K, Ullrich O, Gunzer M, Reymann KG. 2008. Microglia cells protect neurons by direct engulfment of invading neutrophil granulocytes: A new mechanism of CNS immune privilege. J Neurosci 28:5965–5975.

Nimmerjahn A, Kirchhoff F, Helmchen F. 2005. Resting microglial cells are highly dynamic surveillants of brain parenchyma in vivo. Science 308:1314–1318.

Nolte C, Kirchhoff F, Kettenmann H. 1997. Epidermal growth factor is a motility factor for microglial cells in vitro: Evidence for EGF receptor expression. Eur J Neurosci 9:1690–1698.

Ohsawa K, Irino Y, Nakamura Y, Akazawa C, Inoue K, Kohsaka S. 2007. Involvement of $P2X_4$ and $P2Y_{12}$ receptors in ATP-induced microglial chemotaxis. Glia 55:604–616.

Oinuma I, Katoh H, Negishi M. 2006. Semaphorin 4D/Plexin-B1-mediated R-Ras GAP activity inhibits cell migration by regulating beta(1) integrin activity. J Cell Biol 173:601–613.

Simon J, Filippov AK, Goransson S, Wong YH, Frelin C, Michel AD, Brown DA, Barnard EA. 2002. Characterization and channel coupling of the P2Y(12) nucleotide receptor of brain capillary endothelial cells. J Biol Chem 277:31390–31400.

Tadokoro S, Shattil SJ, Eto K, Tai V, Liddington RC, de Pereda JM, Ginsberg MH, Calderwood DA. 2003. Talin binding to integrin beta tails: A final common step in integrin activation. Science 302:103–106.

Tate CC, Garcia AJ, LaPlaca MC. 2007. Plasma fibronectin is neuroprotective following traumatic brain injury. Exp Neurol 207:13–22.

Tsuda M, Shigemoto-Mogami Y, Koizumi S, Mizokoshi A, Kohsaka S, Salter MW, Inoue K. 2003. $P2X_4$ receptors induced in spinal microglia gate tactile allodynia after nerve injury. Nature 424:778–783.

Webb SE, Pollard JW, Jones GE. 1996. Direct observation and quantification of macrophage chemoattraction to the growth factor CSF-1. J Cell Sci 109 (Pt 4):793–803.

Wu LJ, Vadakkan KI, Zhuo M. 2007. ATP-induced chemotaxis of microglial processes requires P2Y receptor-activated initiation of outward potassium currents. Glia 55:810–821.

Zhou FC. 1990. Four patterns of laminin-immunoreactive structure in developing rat brain. Brain Res Dev Brain Res 55:191–201.

Role of PAF Receptor in Proinflammatory Cytokine Expression in the Dorsal Root Ganglion and Tactile Allodynia in a Rodent Model of Neuropathic Pain

Shigeo Hasegawa[1], Yuta Kohro[1], Miho Shiratori[1], Satoshi Ishii[2], Takao Shimizu[2], Makoto Tsuda[1], Kazuhide Inoue[1]*

1 Department of Molecular and System Pharmacology, Graduate School of Pharmaceutical Sciences, Kyushu University, Fukuoka, Japan, **2** Department of Biochemistry and Molecular Biology, Faculty of Medicine, The University of Tokyo, Tokyo, Japan

Abstract

Background: Neuropathic pain is a highly debilitating chronic pain following damage to peripheral sensory neurons and is often resistant to all treatments currently available, including opioids. We have previously shown that peripheral nerve injury induces activation of cytosolic phospholipase A_2 ($cPLA_2$) in injured dorsal root ganglion (DRG) neurons that contribute to tactile allodynia, a hallmark of neuropathic pain. However, lipid mediators downstream of $cPLA_2$ activation to produce tactile allodynia remain to be determined.

Principal Findings: Here we provide evidence that platelet-activating factor (PAF) is a potential candidate. Pharmacological blockade of PAF receptors (PAFRs) reduced the development and expression of tactile allodynia following nerve injury. The expression of PAFR mRNA was increased in the DRG ipsilateral to nerve injury, which was seen mainly in macrophages. Furthermore, mice lacking PAFRs showed a reduction of nerve injury-induced tactile allodynia and, interestingly, a marked suppression of upregulation of tumor necrosis factor α (TNFα) and interleukin-1β (IL-1β) expression in the injured DRG, crucial proinflammatory cytokines involved in pain hypersensitivity. Conversely, a single injection of PAF near the DRG of naïve rats caused a decrease in the paw withdrawal threshold to mechanical stimulation in a dose-dependent manner and an increase in the expression of mRNAs for TNFα and IL-1β, both of which were inhibited by pretreatment with a PAFR antagonist.

Conclusions: Our results indicate that the PAF/PAFR system has an important role in production of TNFα and IL-1β in the DRG and tactile allodynia following peripheral nerve injury and suggest that blocking PAFRs may be a viable therapeutic strategy for treating neuropathic pain.

Citation: Hasegawa S, Kohro Y, Shiratori M, Ishii S, Shimizu T, et al. (2010) Role of PAF Receptor in Proinflammatory Cytokine Expression in the Dorsal Root Ganglion and Tactile Allodynia in a Rodent Model of Neuropathic Pain. PLoS ONE 5(5): e10467. doi:10.1371/journal.pone.0010467

Editor: Louis S. Premkumar, Southern Illinois University School of Medicine, United States of America

Received October 7, 2009; **Accepted** April 10, 2010; **Published** May 3, 2010

Funding: This work was supported by grants from the Ministry of Education, Culture, Sports, Science and Technology of Japan (#20689030 to MT, #18GS0319 to KI). The funders had no role in study design, data collection and analysis, decision to publish, or preparation of the manuscript.

Competing Interests: The authors have declared that no competing interests exist.

* E-mail: inoue@phar.kyushu-u.ac.jp

Introduction

Neuropathic pain that occurs after nerve injury results from an aberrant functioning of a pathologically altered nervous system [1,2]. A hallmark of neuropathic pain syndrome is tactile allodynia, an abnormal hypersensitivity to innocuous stimuli, which is often resistant to all treatments currently available, including potent analgesic opioid drugs. The underlying mechanisms by which nerve injury develops tactile allodynia have remained largely unknown. The dorsal root ganglion (DRG) contains cell bodies of primary afferent neurons that transmit sensory information from the periphery to the central nervous system. The activation of signal transduction cascades and the transcriptional changes in the DRG and the resultant alterations in the transmission properties of sensory neurons following peripheral nerve injury might be involved in modulation of pain signaling in acute and chronic pain conditions [2,3].

We have previously shown that peripheral nerve injury induces activation of cytosolic phospholipase A_2 ($cPLA_2$), a Ca^{2+}-dependent subclass of the PLA_2 family [4] that is required for tactile allodynia [5], in DRG neurons. However, the way in which activated $cPLA_2$ participates in tactile allodynia remains unknown. $cPLA_2$ is a crucial enzyme that catalyzes the hydrolysis of phospholipids to release arachidonic acid and lysophospholipid, and subsequently generates lipid mediators. Arachidonic acid is metabolized to prostaglandins by the cyclooxygenase (COX) pathway and to leukotrienes by the lipoxygenase (LOX) pathway. Lysophospholipid can be converted to platelet-activating factor (PAF) by lyso-PAF acetyltransferase and to lysophosphatidic acid (LPA) by lysophospholipase D. It raises the possibility that these lipid mediators mediated by $cPLA_2$ activation may be secreted from DRG neurons and, in turn, may modulate the excitation of DRG neurons directly or indirectly. Indeed, prostaglandins have been shown to cause sensitization of peripheral sensory neurons

(peripheral sensitization) [6] and to produce allodynic behavior [7,8]. LOX products activate capsaicin receptors in primary sensory neurons, resulting in the induction of peripheral sensitization [9,10]. Furthermore, PAF injected into the hindpaw of naïve animals produces nociceptive responses and mechanical hypersensitivity [11], and recent works have also shown that intrathecal administration of LPA [12] and PAF [13,14] in naïve animals induces tactile allodynia. However, the role of these lipid mediators in the pathogenesis of neuropathic pain is not fully understood.

In the present study, to determine the neuropathic pain-related lipid mediators downstream of $cPLA_2$ activation in the DRG, we investigate the involvement of enzymes and lipid mediator receptors in nerve injury-induced tactile allodynia using pharmacological, molecular, and genetic approaches. We further investigated the role of the lipid mediator receptors in the expression of tumor necrosis factor α (TNFα) and interleukin-1β (IL-1β) in the DRG, proinflammatory cytokines that are strongly implicated in nerve injury-induced tactile allodynia [15,16,17,18].

Results

Effects of COX and LOX inhibitors on the development of tactile allodynia after nerve injury

To determine an involvement of a COX-dependent pathway in tactile allodynia, we first performed double-immunolabeling for phosphorylated-$cPLA_2$ (p-$cPLA_2$) and COX. In the both side of the L5 DRG after nerve injury, COX-1-immunoreactivity (COX-1-IR) was present mainly in small-sized neurons, whereas no COX-2-IR was observed (Fig. 1A), consistent with previous studies [19,20]. Thus, we examined the effect of the selective COX-1 inhibitor SC-560 [21] on the development of nerve injury-induced tactile allodynia. Vehicle-treated rats with an L5 nerve injury displayed a marked decrease in paw withdrawal threshold at the ipsilateral side after nerve injury ($p<0.001$) (Fig. 1B). Similarly, nerve-injured rats that had been treated with SC-560 showed a decreased paw withdrawal threshold ($p<0.001$) and there were no significant differences in the threshold of ipsilateral side between the vehicle- and SC-560-treated group (Fig. 1B). We also found that most of neurons with the translocated p-$cPLA_2$ were not double-labeled with COX-1-IR (169/251, 67.3% of p-$cPLA_2$-translocated neurons) (Fig. 1C). In a small group of DRG neurons, especially small-sized neurons, both types of immunoreactivity were observed, but their subcellular localizations were different: COX-1-IR was observed in the perinuclear area where p-$cPLA_2$-IR was not accumulated (Fig. 1D). Next, to investigate the involvement of LOX in nerve injury-induced tactile allodynia, we examined the effects of the 5-LOX inhibitor AA-861 [22] and the 12- and 15-LOX inhibitor baicalein [23,24] and found that AA-861- and baicalein-treated rats displayed a decrease in paw withdrawal threshold with a similar time course to that of vehicle-treated rats (Fig. 2A, B). There were no significant differences in the threshold between the vehicle- and the LOX inhibitor-treated groups. The doses of the COX and LOX inhibitors used in this study are approximately equivalent to (or even higher than) doses that are known to inhibit behavioral responses mediated by COX [25,26] and LOX [27,28], respectively. Thus, these results suggest that COX and LOX in the DRG may not be involved in nerve injury-induced tactile allodynia.

Effects of PAFR and LPAR antagonists on nerve injury-induced tactile allodynia

To determine the role of lysophospholipid-derived lipid mediators such as PAF and LPA in nerve injury-induced tactile allodynia, we administered PAFR and LPA receptor (LPAR)

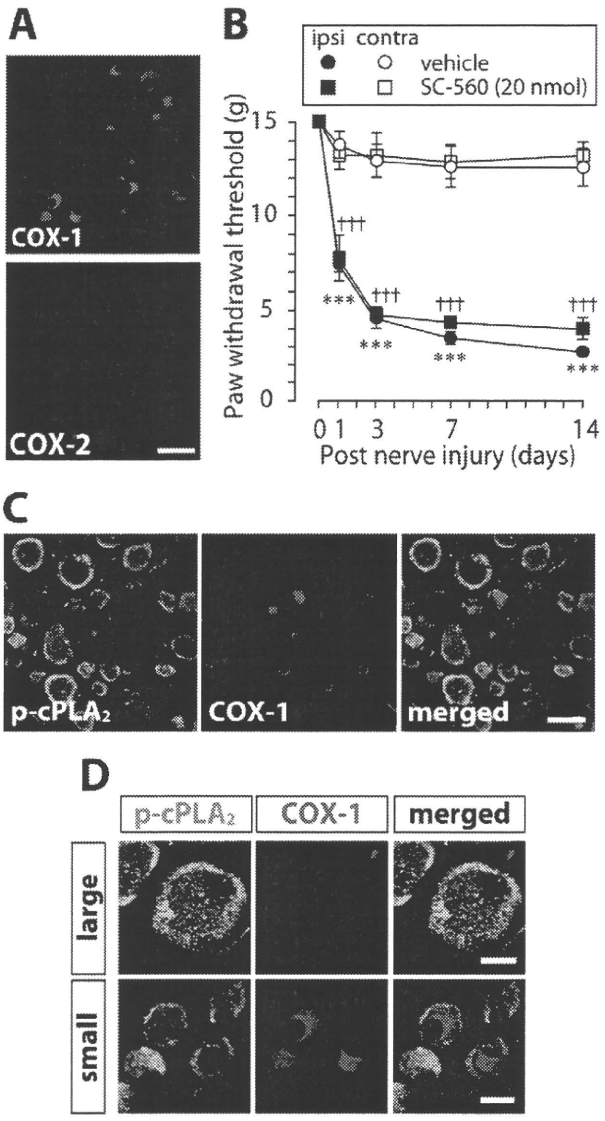

Figure 1. A COX inhibitor does not prevent the development of tactile allodynia after nerve injury. A. Immunofluorescence labeling of COX-1 and COX-2 proteins in the L5 DRG 14 days after nerve injury demonstrated that immunoreactivity of COX-1, but not COX-2, was present mainly in small-sized neurons. Scale bar, 50 μm. B. The COX-1 inhibitor SC-560 (20 nmol/10 μl) administered through a catheter whose tip was positioned near the L5 DRG once daily for 14 days did not suppress the development of nerve injury-induced a decrease in the paw withdrawal threshold of tactile stimulation using von Frey filaments. ***$p<0.001$ compared with the threshold of the vehicle-treated group on day 0. †††$p<0.001$ compared with the threshold of the inhibitor-treated group on day 0. Data are presented as mean ± SEM of the paw withdrawal threshold of five animals. C. Double immunofluorescence labeling of p-$cPLA_2$ with COX-1 in L5 DRG neurons 14 days after nerve injury showed that most of neurons with the translocated p-$cPLA_2$ were not double-labeled with COX-1-IR. Scale bar, 50 μm. D. Highly magnified pictures of large and small diameter DRG neurons demonstrated that in large neurons, p-$cPLA_2$ was not co-expressed with COX-1-IR. In small neurons, the subcellular localizations of p-$cPLA_2$ and COX-1-IR were different: COX-1-immunoreactivity was observed in the perinuclear area where p-$cPLA_2$- immunoreactivity was not accumulated. Scale bars, 20 μm.
doi:10.1371/journal.pone.0010467.g001

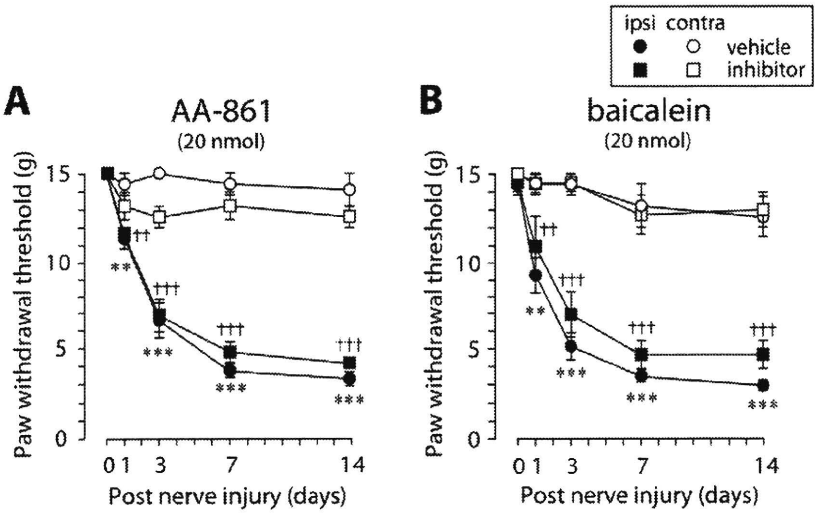

Figure 2. LOX inhibitors do not prevent the development of tactile allodynia after nerve injury. A, B. The 5-LOX inhibitor AA-861 (20 nmol/10 μl) (A) and the 12- and 15-LOX inhibitor baicalein (20 nmol/10 μl) (B) administered through a catheter whose tip was positioned near the L5 DRG once daily for 14 days did not suppressed the development of nerve injury-induced tactile allodynia. $^{**}p<0.01$, $^{***}p<0.001$ compared with the threshold of the vehicle-treated group on day 0. $\dagger\dagger p<0.01$, $\dagger\dagger\dagger p<0.001$ compared with the threshold of the inhibitor-treated group on day 0. All data are presented as mean ± SEM of the paw withdrawal threshold of five animals.
doi:10.1371/journal.pone.0010467.g002

antagonists to nerve-injured rats because inhibitors of PAF and LPA biosynthetic enzymes are not available. We injected the PAFR antagonist CV-3988 [29] and the LPA_1R and LPA_3R antagonist Ki16425 [30] near the L5 DRG and found that CV-3988 and Ki16425 significantly reduced the development of tactile allodynia (CV-3988, $p<0.001$; Ki16425, day 3: $p<0.01$, day 7: $p<0.001$, day 14: $p<0.05$) (Fig. 3A, B). By contrast, such suppressing effect of CV-3988 on allodynia development was not observed when CV-3988 was administered to the lumbar enlargement of the spinal cord (where injured DRG neurons project) (Fig. S1), suggesting that the anti-allodynic effect of the PAFR antagonist may predominantly involve PAFRs expressed in the DRG rather than in the spinal cord. In addition, CV-3988 treatment did not suppress thermal hyperalgesia (Fig. S2). Since our previous study showed that acute inhibition of $cPLA_2$ produces an alleviation of existing tactile allodynia [5], we then examined whether pharmacological blockade of PAFRs and LPARs could also be effective in treating existing allodynia. A single administration of CV-3988 near the DRG 7 days after nerve injury also partially reduced the expression of tactile allodynia within 60 min ($p<0.001$) (Fig. 4A), whereas the decreased paw withdrawal threshold at day 7 after nerve injury was not reversed

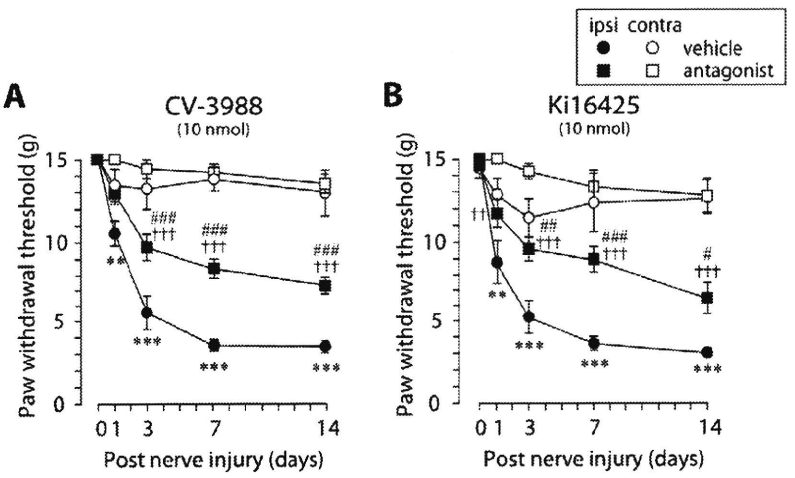

Figure 3. PAFR and LPAR antagonists suppress the development of tactile allodynia by injury to the L5 spinal nerve. A, B. Administration of PAFR antagonist CV-3988 (10 nmol/10 μl) (A) and the LPAR antagonist Ki16425 (10 nmol/10 μl) (B) through a catheter whose tip was positioned near the L5 DRG once daily for 14 days after nerve injury suppressed the development of tactile allodynia. $^{**}p<0.01$, $^{***}p<0.001$ compared with the threshold of the vehicle-treated group on day 0. $\dagger\dagger p<0.01$, $\dagger\dagger\dagger p<0.001$ compared with the threshold of the antagonist-treated group on day 0. $\#p<0.05$, $\#\#p<0.01$, $\#\#\#p<0.001$ compared with the threshold of the vehicle-treated group at each time point. All data are presented as mean ± SEM of the paw withdrawal threshold of five to eight animals.
doi:10.1371/journal.pone.0010467.g003

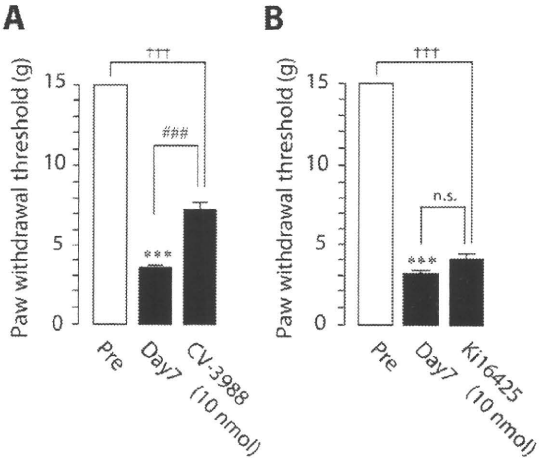

Figure 4. Inhibition of PAFR induces a relieving effect on existing tactile allodynia. A. The decrease in paw withdrawal threshold was attenuated by a single administration of CV-3988 (10 nmol/10 μl) (A), but not Ki16425 (10 nmol/10 μl) (B), through a catheter whose tip was positioned near the L5 DRG on day 7 after nerve injury. ***$p<0.001$, †††$p<0.001$ compared with pre-injury baseline (Pre). ###$p<0.001$ compared with the threshold on day 7. n.s. means "not significant". All data are presented as mean ± SEM of the paw withdrawal threshold of five to eight animals.
doi:10.1371/journal.pone.0010467.g004

by a single administration of Ki16425 (Fig. 4B), consistent with a previous study [12,31]. Alterations in motor behavior after CV-3988 and Ki16425 treatment were not observed (data not shown). These results thus indicate that the PAFR has an important role in the development and maintenance of tactile allodynia whereas the LPAR in the DRG is important only for the development of tactile allodynia.

Lyso-PAF-acetyltransferase LPCAT2 expression in the DRG

Because a mechanism underlying LPAR-mediated tactile allodynia has been previously demonstrated [12,31], in the present study we investigated the role of the PAF-PAFR system in the DRG. First, we examined whether DRG neurons with activated $cPLA_2$ express the lyso-PAF-acetyltransferase LPCAT2, a critical enzyme that produces PAF [32,33,34]. However, it is difficult to perform double-immunolabeling of DRG sections with p-$cPLA_2$ and LPCAT2 antibodies, because they were raised in the same host species (rabbit). Thus, in this experiment, we used two adjacent DRG sections and singly immunostained one section with each antibody. We observed DRG neurons that were positive for both p-$cPLA_2$ and LPCAT2 in the injured DRG 7 days after nerve injury (indicated by arrowheads, Fig. 5). These results suggest that LPCAT2 and activated $cPLA_2$ are co-expressed in the injured DRG. In addition, we observed many small cells that are strongly positive to LPCAT2-IR around DRG neurons, and, surprisingly, these are not overlapped with p-$cPLA_2$-IR (indicated by arrows, Fig. 5). It remains unclear whether the role of LPCAT2 in these small cells in neuropathic pain, and further investigations will be needed to clarify its role.

Upregulation of the PAFR in the DRG after peripheral nerve injury

We next examined the level of PAFR mRNA in total RNA extracts from the L5 DRG ipsilateral and contralateral to an injury

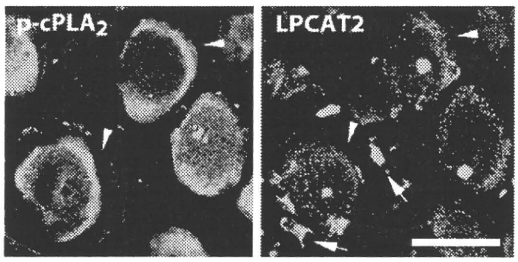

Figure 5. LPCAT2 is expressed in DRG neurons positive to p-cPAL$_2$ following peripheral nerve injury. Immunohistochemical analysis using two adjacent DRG sections (singly immunostained one section with p-$cPLA_2$ or LPCAT2 antibody) revealed that there were DRG neurons positive for both p-$cPLA_2$ and LPCAT2 in the injured DRG (arrowheads) 7 days after nerve injury. Arrows indicate unknown cells that were strongly positive to LPCAT2-IR and negative to p-$cPLA_2$-IR. Scale bar, 50 μm.
doi:10.1371/journal.pone.0010467.g005

to the L5 spinal nerve. We found that the expression of PAFR mRNA in the ipsilateral DRG was markedly increased after nerve injury (Fig. 6A). A significant increase was observed from day 3 after injury ($p<0.01$ compared with the value of the contralateral hindpaw) and PAFR mRNA levels peaked on day 14 (day 7: $p<0.01$, day 14: $p<0.001$ compared with the value of contralateral hindpaw and day 7: $p<0.01$, day 14: $p<0.001$ compared with that of naïve group) (Fig. 6A). The upregulation of PAFR mRNA expression on day 14 was not suppressed by CV-3988 administered for 14 days (116% of the ipsilateral DRG of vehicle-treated rats). In *in situ* hybridization analysis, we found that the intensity of PAFR mRNA signals and the number of cells with strong signal of PAFR mRNA were increased in the ipsilateral DRG 7 days after nerve injury (Fig. 6C) compared with the contralateral DRG (Fig. 6B). The expression of PAFR mRNA was increased in the cells (arrowheads) surrounding DRG neurons (indicated as 'N') in the ipsilateral DRG (Fig. 6C). Such specific signals of PAFR mRNA were not seen in sections hybridized with a corresponding sense probe (Fig. 6D). In addition, we performed *in situ* hybridization using another sets of probes (NM_053321 positioned at 2518-3111 bases), and similar data of PAFR mRNA were observed (data not shown). We validated the hybridization efficiency of antisense and sense probes used in this study with the spleen sections where the PAFR expression is known to be high [35] (Fig. S3). To identify the type of cells expressing PAFR, we performed *in situ* hybridization combined with immunohistochemistry for the macrophages/microglia marker Iba1 (ionized calcium-binding adapter molecule-1) and the satellite cells marker GFAP (glial fibrillary acidic protein). We showed that the PAFR mRNA signals in the injured DRG were restricted to cells labeled with Iba1 (Fig. 6E, arrowheads), but not GFAP (Fig. 6F; GFAP, arrows; PAFR mRNA, arrowheads). These results indicate that PAFR expression in the DRG is upregulated in macrophages after nerve injury.

Attenuation of nerve injury-induced tactile allodynia in *pafr*$^{-/-}$ mice

To precisely determine the functional relevance of PAFR, we used PAFR-deficient mice (*pafr*$^{-/-}$ mice) [36]. *pafr*$^{-/-}$ mice showed no major defects in basal mechanical sensitivity or motor coordination in the rotarod test [37]. Wild-type mice with an L5 nerve injury showed a progressively decreased paw withdrawal threshold (day 1: $p<0.01$, day 3, 7, 10 and 14: $p<0.001$) (Fig. 7). There were significant differences in the threshold between wild-type and *pafr*$^{-/-}$ mice (day 7: $p<0.01$, day 10 and 14: $p<0.05$)

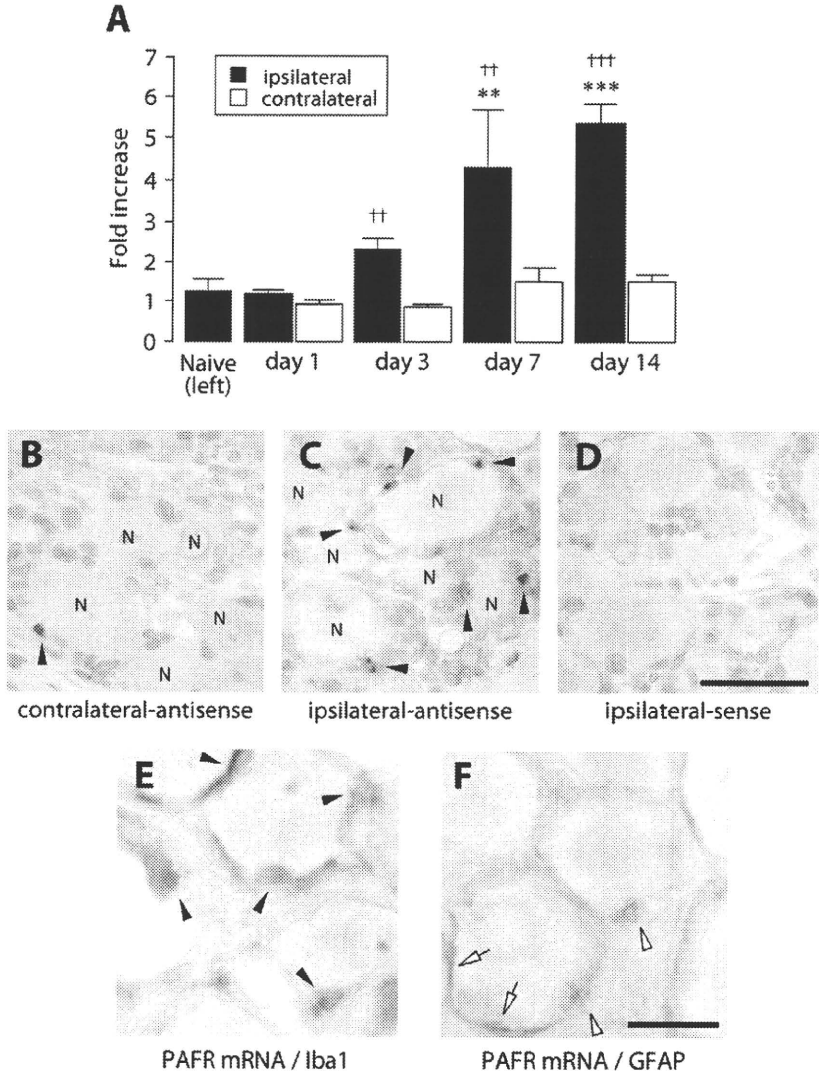

Figure 6. PAFR mRNA is upregulated in the DRG following peripheral nerve injury. A. Real-time PCR analysis revealed that PAFR mRNA expression in total RNA extract from the L5 DRG was markedly increased after peripheral nerve injury. The bar graphs show the average fold increase in the level of PAFR mRNA expression in the DRG compared with the mean expression level of PAFR mRNA in naïve rats. Each measurement was normalized to GAPDH content. $^{**}p<0.01$, $^{***}p<0.001$ compared with naïve rats. $\dagger\dagger p<0.01$, $\dagger\dagger\dagger p<0.001$ compared with the contralateral side. All data are presented as mean ± SEM of five individual animals. B-D. DIG-labeled antisense (B: contralateral, C: ipsilateral) and sense (D: ipsilateral) probes specific for PAFR mRNA were visualized by *in situ* hybridization in the rat DRG 7 days after nerve injury. Strong PAFR mRNA signals were observed in the cells surrounding DRG neurons in the ipsilateral DRG 7 days after nerve injury. Arrowheads show PAFR mRNA-positive cells. 'N' indicates neuronal cells. Similar results were observed in each of three experiments. Scale bar, 50 μm. E,F. *In situ* hybridization combined with immunohistochemistry for the macrophages/microglia marker Iba1 and the satellite glia marker GFAP was performed. PAFR mRNA signals overlapped with Iba1-IR (arrowheads, E) but not with GFAP-IR (GFAP: white arrowheads, PAFR: white arrows, F). Scale bar, 25 μm.
doi:10.1371/journal.pone.0010467.g006

even though the threshold in *pafr*$^{-/-}$ mice was decreased after injury (Fig. 7). Ablation of PAFRs did not change the paw withdrawal threshold at the side contralateral to the nerve injury (Fig. 7). Thus, PAFR might be required for tactile allodynia following peripheral nerve injury.

Reduction of upregulation of TNFα and IL-1β expression in *pafr*$^{-/-}$ mice

TNFα and IL-1β are proinflammatory cytokines that have been reported to be upregulated in the DRG following peripheral nerve injury [16,17,38] and be produced via PAFRs in non-neuronal cells [39,40]. We predicted that the loss of PAFRs could affect the levels of TNFα and IL-1β in the L5 DRG. To address this, we examined the levels of mRNA of these cytokines in the DRG after nerve injury using real-time RT-PCR. The expression levels of these mRNAs at the ipsilateral DRG of wild-type mice was much higher than at the contralateral side on day 7 (TNFα: $p<0.01$, IL-1β: $p<0.001$) (Fig. 8A, B), but *pafr*$^{-/-}$ mice failed to show upregulation of these cytokines and there were significant differences in these expression level of ipsilateral side between wild-type and *pafr*$^{-/-}$ mice (TNFα: $p<0.05$, IL-1β: $p<0.01$).

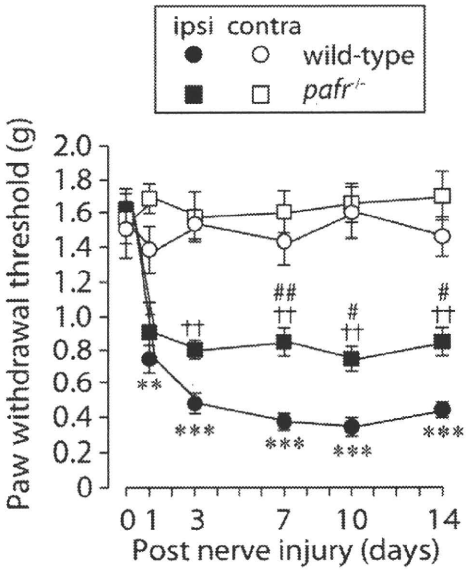

Figure 7. Deletion of *pafr* reduces tactile allodynia. While wild-type mice with an L5 nerve injury showed a progressively decreased paw withdrawal threshold, $pafr^{-/-}$ mice showed an attenuation of the decrease in paw withdrawal threshold after nerve injury. $^{**}p<0.01$, $^{***}p<0.001$ compared with the threshold of wild-type mice on day 0. $\dagger\dagger p<0.01$ compared with the threshold of $pafr^{-/-}$ mice on day 0. $\#p<0.05$, $\#\#p<0.01$ compared with the threshold of the wild-type mice at each time point. All data are presented as mean ± SEM of six to eight animals.
doi:10.1371/journal.pone.0010467.g007

Ablating PAFRs did not change cytokine expression at the contralateral DRG. These results indicate that PAFRs might contribute to tactile allodynia via TNFα and IL-1β production in the DRG following nerve injury.

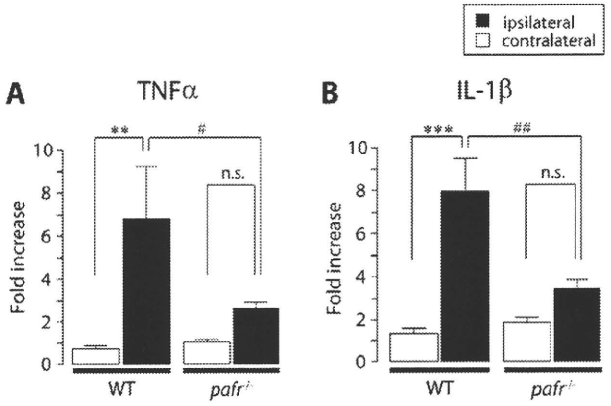

Figure 8. Upregulation of TNFα and IL-1β gene expression in the DRG is reduced in $pafr^{-/-}$ mice. A, B. Real-time PCR analysis demonstrated that following nerve injury, the expression of TNFα (A) and IL-1β (B) mRNAs in the ipsilateral DRG of wild-type mice was much higher than in the contralateral side on day 7. However, $pafr^{-/-}$ mice failed to show upregulation of these cytokines and there were significant differences in these expressions of the ipsilateral side between wild-type and $pafr^{-/-}$ mice. Each measurement was normalized to 18S mRNA content. $^{**}p<0.01$, $^{***}p<0.001$ compared with the contralateral side of wild-type mice. $\#p<0.05$, $\#\#p<0.01$ compared with the ipsilateral side. n.s. means "not significant". All data are presented as mean ± SEM of six to eight animals.
doi:10.1371/journal.pone.0010467.g008

Effect of PAF injection on paw withdrawal threshold and cytokine production in the DRG

We determined whether injection of PAF in the absence of nerve injury is sufficient to produce tactile allodynia and to upregulate cytokine expression in the DRG. A single injection of PAF near the DRG of naïve rats caused a decrease in the paw withdrawal threshold to mechanical stimulation in a dose-dependent manner (Fig. 9A). The threshold began to decrease 15 min after PAF injection and peaked at 45–60 min, then gradually recovered over 4 h (Fig. 9A). The decrease in the withdrawal threshold induced by PAF was inhibited by pretreatment with CV-3988 ($p<0.01$) (Fig. 9B). We then performed real-time RT-PCR analysis using the DRG of rats that had been injected with PAF. The expression of mRNAs for TNFα and IL-1β was increased 45 min after PAF injection (Fig. 9C, D), when the threshold was markedly reduced. This effect was also prevented by pretreatment with CV-3988 (Fig. 9C, D). These results suggest that administering PAF near the DRG causes a decrease in the withdrawal threshold and production of TNFα and IL-1β via PAFR.

Discussion

In the present study, we provide the first evidence that in the DRG, PAFR is important in the pathogenesis of tactile allodynia, a major behavioral consequence of nerve injury, and are responsible for production of proinflammatory cytokines such as TNFα and IL-1β.

We have previously shown that $cPLA_2$ is translocated to the plasma membrane mainly in medium- to large-diameter DRG neurons [5], but COX-1 was present around the perinuclear region of small-sized DRG neurons. In addition, our behavioral studies demonstrated that administering the COX-1 inhibitor SC-560 near the injured DRG showed no anti-allodynic effect at doses that are considered to inhibit this enzyme [25,26]. A previous study reported that administration of SC-560 to the lumbar enlargement of the spinal cord at a higher dose than our study prevented a decrease in the paw withdrawal threshold after nerve injury [41], which seems to be partly inconsistent with our present results. However, peripheral nerve injury causes an increase in COX-1 and COX-2 expression in the spinal cord [42,43], but not in the DRG, and a high dose of SC-560 also slightly inhibits COX-2 [21]. Thus, it is possible that the discrepancy in the effect of SC-560 on tactile allodynia might be explained by the difference in dose and region of drug administration. These results thus suggest that COX in the DRG is not primarily involved in the $cPLA_2$-dependent tactile allodynia. These data may also provide a putative explanation for the resistance or controversial effects of COX inhibitors on allodynic behavior reported in both animals and patients with neuropathic pain [44].

Similar to SC-560, neither the 5-LOX inhibitor AA-861 nor the 12- and 15-LOX inhibitor baicalein showed the inhibitory effect on nerve injury-induced tactile allodynia. Products of lipoxygenases such as leukotrienes, hydroxyeicosatetraenoic acids (HETEs) and hydroperoxyeicosatetraenoic acids (HPETEs) have been implicated in mediating inflammatory nociception because they are produced during inflammation [45] and cause hyperalgesia when injected intradermally [46,47], but so far there have been no reports that clearly show the involvement of lipoxygenases in tactile allodynia. These findings and the data presented here suggest that in the DRG, LOX does not also play a major role in nerve injury-induced tactile allodynia as in the case of COX, while we can not completely exclude the possibility that COX and LOX in the spinal cord are involved in tactile

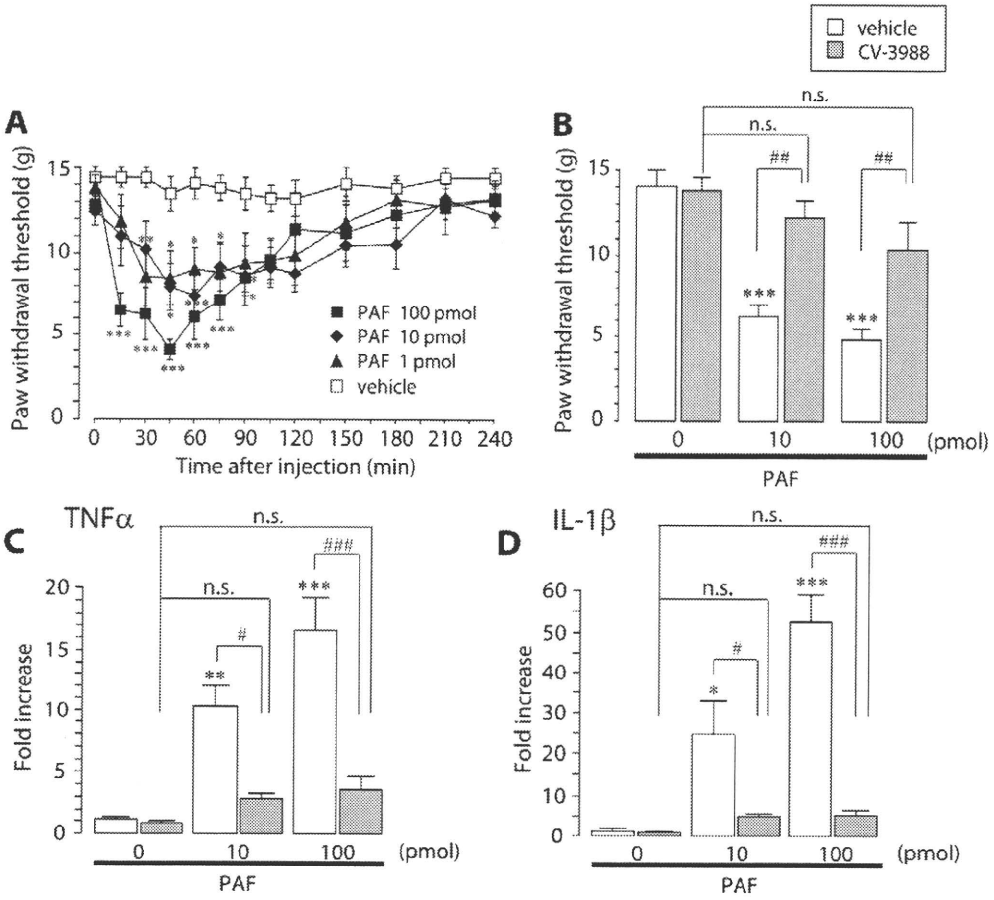

Figure 9. Injection of PAF near the DRG induces a decrease in the paw withdrawal threshold and upregulation of TNFα and IL-1β mRNAs. A. Paw withdrawal threshold was decreased by single administration of several different doses of PAF near the DRG in normal rats. *$p<0.05$, **$p<0.01$, ***$p<0.001$ compared with the threshold of the vehicle-treated group. B. The PAF-induced decrease in paw withdrawal threshold was suppressed by pretreatment with CV-3988. ***$p<0.001$ compared with the threshold of the vehicle-treated group. ##$p<0.01$ compared with the threshold of the PAF-treated group. n.s. means "not significant". C, D. Real-time PCR analysis showed that administration of PAF near the DRG increased expression of TNFα (C) and IL-1β (D) mRNAs in the DRG 45 min after the administration. The bar graphs show the average fold increase in the level of TNFα and IL-1β mRNAs in the DRG compared with the mean expression level of these mRNAs in the vehicle-treated group. Each measurement was normalized to 18S mRNA content. *$p<0.05$, **$p<0.01$, ***$p<0.001$ compared with the vehicle-treated group. #$p<0.05$, ###$p<0.001$ compared with the PAF-treated group. n.s. means "not significant". All data are presented as mean ± SEM of four to six animals.
doi:10.1371/journal.pone.0010467.g009

allodynia. Furthermore, because COX-1 expression was observed mainly in small-diameter DRG neurons and LOX products activate capsaicin receptors in primary sensory neurons [9,10], COX and LOX in the DRG may participate in thermal hyperalgesia after nerve injury.

The crucial role of PAFR in neuropathic pain was demonstrated for the first time by the data obtained from the behavioral analyses using pharmacological and genetic tools. Administration of the PAFR antagonist CV-3988 near the injured DRG reduced the development and expression of nerve injury-induced tactile allodynia. By contrast, the reducing effect of the development of tactile allodynia by administration of CV-3988 to the lumbar enlargement of the spinal cord was much less than that by injection of the antagonist near the DRG. Furthermore, DRG neurons with activated $cPLA_2$ also expressed the lyso-PAF-acetyltransferase LPCAT2, a critical enzyme that produces PAF [32,33,34]. Our data from real-time RT-PCR analyses showed that PAFR gene expression was increased in the ipsilateral DRG after nerve injury. These findings thus suggest that the PAF/PAFR system may be activated in the injured DRG and contribute to nerve injury-induced tactile allodynia, although a possible involvement of PAFR in the spinal cord can not be completely excluded [13]. Moreover, our *in situ* hybridization experiments revealed that following peripheral nerve injury a marked increase in PAFR mRNA expression was seen mainly in non-neuronal cells positive to Iba1. It is conceivable that peripheral nerve injury causes the transcriptional upregulation of PAFR in macrophages in the DRG. Alternatively, infiltration of macrophages expressing PAFR in the DRG after nerve injury might result in the upregulation of PAFR mRNA, because PAFR is expressed in macrophages [35] and is involved in macrophage chemotaxis [48] and the number of macrophages in the DRG is increased following peripheral nerve injury [49]. Interestingly, PAFR-deficient mice showed a marked suppression of the upregulation of TNFα and IL-1β expression in the injured DRG. This is consistent with the notion that macrophages are one of the major sources of these proinflammatory cytokines and regulate pain signaling [49,50,51,52], although it remains unknown whether PAFR activation leads to upregulation of proinflammatory cytokine expression in macrophages.

It has been reported that TNFα [38,53,54,55,56] and IL-1β [16,17] are upregulated in the DRG following peripheral nerve injury and are implicated in tactile allodynia. Increased synthesis and release of TNFα and IL-1β can directly modulate neuronal activity and elicit spontaneous action potential discharges in the DRG [49]. TNFα enhances tetrodotoxin-resistant Na^+ currents in DRG neurons through TNF receptor 1 [57]. Both injured and adjacent uninjured primary afferent neurons become more sensitive to TNFα after spinal nerve ligation [18]. Similarly, IL-1β application has been shown to increase the excitability of sensory neurons by potentiating voltage-dependent Na^+ currents [58]. Therefore, these cytokines in the injured DRG might be involved in sensitization of primary sensory neurons that link to nerve injury-induced tactile allodynia. It remains unclear whether the expression of these cytokines results from PAFR activation in non-neuronal cells in the DRG. In the future, by generating using cell type-specific PAFR-knockout mice, and by studying their phenotypes, this issue will be determined.

LPA could also be a candidate signaling molecule that is responsible for nerve injury-induced tactile allodynia. Our behavioral study demonstrated that injection of the LPAR antagonist Ki16425 near the injured DRG reduced the development, but not maintenance, of tactile allodynia, which is consistent with a previous study [12]. Because among LPARs, LPA_1R is mainly expressed in the DRG and LPA_1R-deficient mice attenuate nerve injury-induced tactile allodynia [12]. LPA_1Rs mediate demyelination and upregulate the expression of the $\alpha_2\delta_1$ subunit of the voltage-gated calcium channel in the DRG [12], and these might be the mechanisms underlying LPA-dependent tactile allodynia. Furthermore, LPA increases the intracellular calcium concentration in adult DRG neurons [59] and intraplantar injection of LPA causes a nociceptive flexor response [60], suggesting that LPA could produce direct effects on primary afferent neurons and modulate nociceptive responses.

Based on the results obtained from our present and previous studies, we proposed the following mechanism (Fig. 10). After peripheral nerve injury, $cPLA_2$ is activated by Ca^{2+} signaling evoked by P2X3 or P2X2/3 receptors (subtype of ionotropic purinergic receptors) [5]. These receptors are activated by extracellular ATP, which presumably released from neighboring cells such as satellite glia. Activity of voltage-gated Ca^{2+} channels (VDCC) is also involved in $cPLA_2$ activation [61]. The Ca^{2+}-dependent $cPLA_2$ activation is mediated by Ca^{2+}/calmodulin-dependent protein kinase II (CaMKII) [61]. $cPLA_2$ supply lyso-PAF, a precursor of PAF, which in turn converts into PAF by LPCAT2 (although the role of LPCAT2 expressed in unknown cells in the DRG remains unclear). PAF may be released from DRG neurons and then activates PAFR expressed in macrophages. Activation of PAFR may lead to production and release of proinflammatory cytokines. These cytokines increase the excitability of DRG neurons that link to nerve injury-induced tactile allodynia.

In summary, the present study provided the first evidence that the activation of the PAFR may be a key event in the development and maintenance of tactile allodynia and production of proinflammatory cytokines such as TNFα and IL-1β in the DRG. Thus, blocking the PAFR might be a new therapeutic target for treating neuropathic pain. Importantly, basal pain sensitivity was not altered in *pafr*$^{-/-}$ mice, suggesting the possibility of a therapeutic benefit of blocking PAFRs in the treatment of tactile allodynia without affecting normal pain sensitivity. As the PAFR has been implicated in other neurodegenerative disorders such as ischemia [62] and multiple sclerosis [39], interfering with PAFRs could be a therapeutic strategy widely applicable to central nervous system diseases.

Materials and Methods

All animal experiments were conducted according to relevant national and international guidelines 'Act on Welfare and Management of Animals' (Ministry of Environment of Japan) and 'Regulation of Laboratory Animals' (Kyushu University), and under the protocols approved by the Institutional Animal Care and Use committee review panels at Kyushu University and The University of Tokyo.

Animals

Male Wistar rats (250–270 g, Japan SLC, Shizuoka, Japan) and wild-type and *pafr*$^{-/-}$ mice [36] were used. Animals were housed in individual and groups of 2~3 per cage at a temperature of 22±1°C with a 12-h light-dark cycle (light on 8:30 to 20:30), and fed food and water ad libitum.

Neuropathic pain model

We used the spinal nerve injury model [63] with some modifications [64]: in male Wistar rats a unilateral L5 spinal nerve was tightly ligated and cut just distal to the ligature. For the experiments using mice, the left L5 spinal nerve was transected [65]. The mechanical allodynia was assessed by using calibrated von Frey filaments (0.4–15.1 g for rats, 0.02–2.0 g for mice; Stoelting, Wood Dale, IL, USA) and the paw withdrawal threshold was determined as described previously [64].

Drug treatment

Rats were implanted with catheters for drug injection near the L5 DRG according to the method described previously [64,65]. Under isoflurane anesthesia, a sterile 32 gauge catheter (ReCathCo, Allison Park, PA, USA) was inserted into the intrathecal space through the atlanto-occipital membrane and to the L4 or L5 DRG and externalized through the skin [5]. After the experiments, we confirmed that the tip of the catheter was positioned near the L5 DRG. Rats were injected with each drug through the catheter using a 25 μl Hamilton syringe with a 30-gauge needle once a day from day 0 (just before the nerve injury) to day 13. The drugs used in this study are listed below: SC-560 (20 nmol/10 μl, Calbiochem, San Diego, CA, USA), AA-861 (20 nmol/10 μl, Sigma, St Louis, MO, USA), baicalein (20 nmol/10 μl, Calbiochem), CV-3988 (10 nmol/10 μl, Biomol, Plymouth Meeting, PA, USA) and Ki16425 (10 nmol/10 μl, Sigma). The paw withdrawal threshold was tested 21–24 hr after the injection of each drug at 1, 3, 7 and 14 days post-injury. For the experiment in which the effect of a single administration of CV-3988 or Ki16425 on the established allodynia was examined on day 7 after nerve injury, behavioral test was performed immediately before and after the injection of CV-3988 (10 nmol/10 μl) or Ki16425 (10 nmol/10 μl). To examine the effect of PAF on pain behavior, the paw withdrawal threshold was assessed before and after a single injection of PAF near the DRG of naïve rats. Rats were injected with CV-3988 (10 nmol/10 μl) through the catheter 10 min before the injection of PAF.

Immunohistochemistry

Rats were deeply anesthetized by pentobarbital (100 mg/kg, i.p.) and perfused transcardially with 4% paraformaldehyde. DRG sections were removed, postfixed with the same fixative, and placed in 30% sucrose solution for 24 hr at 4°C. The DRG sections (15 μm) were incubated in a blocking solution [3% normal goat serum/0.3% Triton X-100/phosphate-buffered saline (PBS) (−)] and then with anti-phospho-$cPLA_2$ (anti-p-$cPLA_2$) antibody (1:1000, Cell Signaling, Beverly, MA, USA), anti-

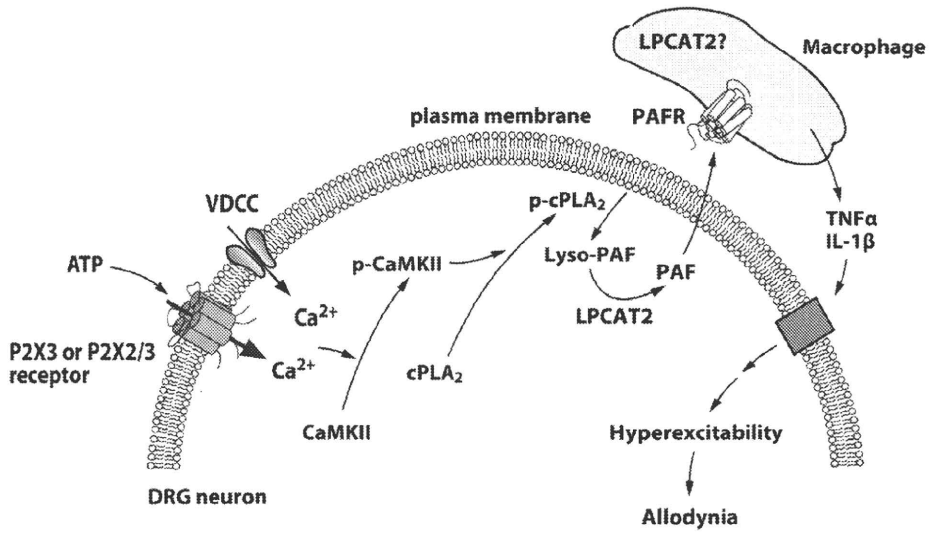

Figure 10. Schematic representation of the proposed mechanism underlying the PAF/PAFR system-mediated neuropathic pain after peripheral nerve injury. After peripheral nerve injury, $cPLA_2$ is activated by Ca^{2+} signaling evoked by P2X3 or P2X2/3 receptors (subtype of ionotropic purinergic receptors) and voltage-gated Ca^{2+} channels (VDCC). The Ca^{2+}-dependent $cPLA_2$ activation involves Ca^{2+}/calmodulin-dependent protein kinase II (CaMKII). $cPLA_2$ supply lyso-PAF which in turn converts into PAF by the lyso-PAF-acetyltransferase LPCAT2. PAF activates PAFR expressed in macrophages. Activation of PAFR may lead to production and release of proinflammatory cytokines, TNFα and IL-1β. These cytokines may increase the excitability of DRG neurons that link to nerve injury-induced tactile allodynia.
doi:10.1371/journal.pone.0010467.g010

COX-1 antibody (1:50, Cayman chemical, Ann Arbor, MI, USA), anti-COX-2 antibody (1:50, Cayman chemical), and anti-LPCAT2 antibody (1:500, [34]). Identification of neurons was performed with a marker of neurons, microtubule associated protein 2 (1:1000, Chemicon, Temecula, CA, USA). Following incubation, the DRG sections were incubated with anti-rabbit immunoglobulin G (IgG)-conjugated Alexa Fluor 488 or anti-mouse IgG-conjugated Alexa Fluor 546 (1:1000, Molecular Probes, Eugene, OR, USA). The sections were then analyzed by a confocal microscope (LSM510, Zeiss, Oberkochen, Germany). DRG neurons were characterized as small (<600 μm^2), medium (600-1200 μm^2), and large (>1200 μm^2)-sized neurons according to their cross-sectional areas [66].

Real-time reverse transcription-PCR

Rats and mice were deeply anesthetized with pentobarbital, perfused transcardially with PBS, and the L5 DRG was removed immediately. Total RNA from the L5 DRG was extracted by using Trisure (Bioline, Danwon-Gu, Korea) according to manufacturer's protocol and purified using RNeasy mini plus kit (QIAGEN, Valencia, CA, USA). The amount of total RNA was quantified by measuring OD_{260} using a Nanodrop spectrophotometer (Nanodrop, Wilmington, DE). For reverse transcription, 100 ng of total RNA was transferred to the reaction with Prime Script reverse transcriptase (Takara, Kyoto, Japan) and random 6-mer primers. Quantitative PCR was carried out with Premix Ex Taq (Takara) using a 7500 real-time PCR system (Applied Biosystems, Foster City, CA) according to protocol of the manufacturer, and the data were analyzed by 7500 System SDS Software 1.3.1 (Applied Biosystems) using the standard curve method. The TaqMan probe, forward primer and reverse primer used in this study were designed as follows: rat PAFR, probe, 5′-FAM- ATCTCACCGTGGCG-GACCTGCTCT-TAMRA-3′, forward, 5′-CCCGTCCAAGAA-ACTGAATGAG-3′, and reverse, 5′-TCGCCCTCGTTGGAG-TAATAGA-3′; mouse TNFα, probe, 5′-FAM-TACGTGCTCCT-CACCCACACCGTCA-TAMRA-3′, forward, 5′-GTTCTCTT-CAAGGGACAAGGCTG-3′, and reverse, 5′-TCCTGGTATGA-GATAGCAAATCGG-3′; mouse IL-1β, probe, 5′-FAM-TGC-AGCTGGAGAGTGTGGATCCCAA-TAMRA-3′, forward, 5′-GAAAGACGGCACACCCACC-3′, and reverse, 5′-AGACAA-ACCGCTTTTCCATCTTC-3′; rat TNFα, probe, 5′-FAM-CGT-AGCCCACGTCGTA-TAMRA-3′, forward, 5′-GACCCTCA-CACTCAGATCATCTTCT-3′, and reverse, 5′- GGTACAGCC-CATCTGCTGGTA-3′; rat IL-1β, probe, 5′-FAM-TCTCCA-CCTCAATGGACAGAACATAAGCCA-TAMRA-3′, forward, 5′-AAATGCCTCGTGCTGTCTGA-3′, and reverse, 5′-GTCG-TTGCTTGTCTCTCCTTGTAC-3′. The primers and probe for GAPDH and 18S mRNA were obtained from Applied Biosystems.

In situ hybridization

Digoxigenin (DIG)-labeled sense and antisense RNA probes were prepared from the sequence of rat *pafr* mRNA (GenBank accession number: NM_053321) positioned at 1178–1819 bases. Rats were anesthetized and perfused transcardially with Tissue Fixative (Genostaff, Tokyo, Japan) 7 day after nerve injury. DRG sections were removed and again fixed with the same fixative. Paraffin-embedded tissues (6 μm) were dewaxed with xylene and rehydrated. After proteinase K treatment (8 μg/ml, 30 min, 37°C) and acetylation by acetic anhydride (0.25%), hybridization was performed with sense and antisense probes at concentrations of 300 ng/ml at 60°C for 16 h. After hybridization, a series of washing was performed, followed by RNase treatment (50 mg/ml, 30 min, 37°C). The sections were blocked with 0.5% blocking reagent (Roche, Indianapolis, IN, USA) in Tris-buffered saline containing Tween 20 and incubated with anti-DIG alkaline phosphatase conjugate (1:1000, Roche) for 2 h at room temperature. Coloring reactions were performed with nitro blue tetrazolium chloride/5-bromo-4-chloro-3-indolyl phosphate solution (NBT/BCIP) (Sigma, St. Louis, MO, USA) overnight. The sections were counterstained with Kernechtrot stain solution (Mutoh, Tokyo, Japan) and then mounted with Malinol (Mutoh). Non-neuronal and neuronal cells with a higher violet intensity

than the sections hybridized with sense probe were considered positively labeled for PAFR mRNA. For immunohistochemistry as a second staining after ISH, the sections were treated 3% hydrogen peroxide in PBS for 15 min, and Protein Block (Dako). Sections were incubated either with the anti-Iba1 rabbit polyclonal antibody (1:1000, Wako) or anti-GFAP rabbit polyclonal antibody (1:500, Dako) at 4°C for overnight. After washing with TBS, sections were incubated with biotin-conjugated goat anti-rabbit IgG (Dako) for 30 min at room temperature, followed by the addition of peroxidase conjugated streptavidin (Nichirei) for 5 min. Peroxidase activity was visualized by diaminobenzine.

Statistical analysis

All data are presented as means ± SEM. The statistical significance of difference between values was determined by Student's *t* test or analysis of variance (ANOVA) with appropriate *post hoc* tests. A *p* value less than 0.05 was considered to be statistically significant.

Supporting Information

Figure S1 The effect of the PAFR antagonist CV-3988 administered to the lumbar enlargement of the spinal cord on the development of nerve injury-induced tactile allodynia. The paw withdrawal threshold of tactile stimulation was examined using von Frey filaments. CV-3988 or vehicle was administered once daily for 7 days. ***$p<0.001$, #$p<0.05$ compared with pre-injury baseline (Pre). n.s. means "not significant". All data are presented as mean ± SEM of the paw withdrawal threshold of three animals.
Found at: doi:10.1371/journal.pone.0010467.s001 (0.06 MB TIF)

Figure S2 PAFR antagonist CV-3988 does not suppress the development of thermal hyperalgesia induced by injury to the L5 spinal nerve. CV-3988 (10 nmol/10 μl) was administered near the DRG once daily for 14 days after nerve injury. *$p<0.05$, **$p<0.01$. All data are presented as mean ± SEM of the paw withdrawal latency to thermal stimulus of four to five rats.
Found at: doi:10.1371/journal.pone.0010467.s002 (0.05 MB TIF)

Figure S3 Validation of digoxigenin-labeled antisense (left) and sense (right) RNA probes prepared from the sequence of rat pafr mRNA (NM_053321 positioned at 1178-1819 bases) with the spleen sections. Scale bar, 25 μm.
Found at: doi:10.1371/journal.pone.0010467.s003 (1.14 MB TIF)

Author Contributions

Conceived and designed the experiments: SH MT KI. Performed the experiments: SH YK MS. Analyzed the data: SH YK. Contributed reagents/materials/analysis tools: SI TS. Wrote the paper: SH MT KI.

References

1. Woolf CJ, Mannion RJ (1999) Neuropathic pain: aetiology, symptoms, mechanisms, and management. Lancet 353: 1959–1964.
2. Woolf CJ, Salter MW (2000) Neuronal plasticity: increasing the gain in pain. Science 288: 1765–1769.
3. Scholz J, Woolf CJ (2002) Can we conquer pain? Nat Neurosci 5 Suppl: 1062–1067.
4. Shimizu T, Ohto T, Kita Y (2006) Cytosolic phospholipase A2: biochemical properties and physiological roles. IUBMB Life 58: 328–333.
5. Tsuda M, Hasegawa S, Inoue K (2007) P2X receptors-mediated cytosolic phospholipase A2 activation in primary afferent sensory neurons contributes to neuropathic pain. J Neurochem 103: 1408–1416.
6. Park KA, Vasko MR (2005) Lipid mediators of sensitivity in sensory neurons. Trends Pharmacol Sci 26: 571–577.
7. Minami T, Uda R, Horiguchi S, Ito S, Hyodo M, et al. (1992) Allodynia evoked by intrathecal administration of prostaglandin F2 alpha to conscious mice. Pain 50: 223–229.
8. Minami T, Uda R, Horiguchi S, Ito S, Hyodo M, et al. (1994) Allodynia evoked by intrathecal administration of prostaglandin E2 to conscious mice. Pain 57: 217–223.
9. Hwang SW, Cho H, Kwak J, Lee SY, Kang CJ, et al. (2000) Direct activation of capsaicin receptors by products of lipoxygenases: endogenous capsaicin-like substances. Proc Natl Acad Sci U S A 97: 6155–6160.
10. Shin J, Cho H, Hwang SW, Jung J, Shin CY, et al. (2002) Bradykinin-12-lipoxygenase-VR1 signaling pathway for inflammatory hyperalgesia. Proc Natl Acad Sci U S A 99: 10150–10155.
11. Marotta DM, Costa R, Motta EM, Fernandes ES, Medeiros R, et al. (2009) Mechanisms underlying the nociceptive responses induced by platelet-activating factor (PAF) in the rat paw. Biochem Pharmacol 77: 1223–1235.
12. Inoue M, Rashid MH, Fujita R, Contos JJ, Chun J, et al. (2004) Initiation of neuropathic pain requires lysophosphatidic acid receptor signaling. Nat Med 10: 712–718.
13. Morita K, Morioka N, Abdin J, Kitayama S, Nakata Y, et al. (2004) Development of tactile allodynia and thermal hyperalgesia by intrathecally administered platelet-activating factor in mice. Pain 111: 351–359.
14. Morita K, Kitayama T, Morioka N, Dohi T (2008) Glycinergic mediation of tactile allodynia induced by platelet-activating factor (PAF) through glutamate-NO-cyclic GMP signalling in spinal cord in mice. Pain 138: 525–536.
15. Schafers M, Svensson CI, Sommer C, Sorkin LS (2003) Tumor necrosis factor-alpha induces mechanical allodynia after spinal nerve ligation by activation of p38 MAPK in primary sensory neurons. J Neurosci 23: 2517–2521.
16. Mika J, Korostynski M, Kaminska D, Wawrzczak-Bargiela A, Osikowicz M, et al. (2008) Interleukin-1alpha has antiallodynic and antihyperalgesic activities in a rat neuropathic pain model. Pain 138: 587–597.
17. Kawasaki Y, Xu ZZ, Wang X, Park JY, Zhuang ZY, et al. (2008) Distinct roles of matrix metalloproteases in the early- and late-phase development of neuropathic pain. Nat Med 14: 331–336.
18. Schafers M, Lee DH, Brors D, Yaksh TL, Sorkin LS (2003) Increased sensitivity of injured and adjacent uninjured rat primary sensory neurons to exogenous tumor necrosis factor-alpha after spinal nerve ligation. J Neurosci 23: 3028–3038.
19. Chopra B, Giblett S, Little JG, Donaldson LF, Tate S, et al. (2000) Cyclooxygenase-1 is a marker for a subpopulation of putative nociceptive neurons in rat dorsal root ganglia. Eur J Neurosci 12: 911–920.
20. Dou W, Jiao Y, Goorha S, Raghow R, Ballou LR (2004) Nociception and the differential expression of cyclooxygenase-1 (COX-1), the COX-1 variant retaining intron-1 (COX-1v), and COX-2 in mouse dorsal root ganglia (DRG). Prostaglandins Other Lipid Mediat 74: 29–43.
21. Smith CJ, Zhang Y, Koboldt CM, Muhammad J, Zweifel BS, et al. (1998) Pharmacological analysis of cyclooxygenase-1 in inflammation. Proc Natl Acad Sci U S A 95: 13313–13318.
22. Yoshimoto T, Yokoyama C, Ochi K, Yamamoto S, Maki Y, et al. (1982) 2,3,5-Trimethyl-6-(12-hydroxy-5,10-dodecadiynyl)-1,4-benzoquinone (AA861), a selective inhibitor of the 5-lipoxygenase reaction and the biosynthesis of slow-reacting substance of anaphylaxis. Biochim Biophys Acta 713: 470–473.
23. Cho H, Ueda M, Tamaoka M, Hamaguchi M, Aisaka K, et al. (1991) Novel caffeic acid derivatives: extremely potent inhibitors of 12-lipoxygenase. J Med Chem 34: 1503–1505.
24. Sadik CD, Sies H, Schewe T (2003) Inhibition of 15-lipoxygenases by flavonoids: structure-activity relations and mode of action. Biochem Pharmacol 65: 773–781.
25. Ririe DG, Prout HD, Barclay D, Tong C, Lin M, et al. (2006) Developmental differences in spinal cyclooxygenase 1 expression after surgical incision. Anesthesiology 104: 426–431.
26. Zhu X, Conklin D, Eisenach JC (2003) Cyclooxygenase-1 in the spinal cord plays an important role in postoperative pain. Pain 104: 15–23.
27. Trang T, McNaull B, Quirion R, Jhamandas K (2004) Involvement of spinal lipoxygenase metabolites in hyperalgesia and opioid tolerance. Eur J Pharmacol 491: 21–30.
28. Trang T, Sutak M, Quirion R, Jhamandas K (2003) Spinal administration of lipoxygenase inhibitors suppresses behavioural and neurochemical manifestations of naloxone-precipitated opioid withdrawal. Br J Pharmacol 140: 295–304.
29. Terashita Z, Tsushima S, Yoshioka Y, Nomura H, Inada Y, et al. (1983) CV-3988 - a specific antagonist of platelet activating factor (PAF). Life Sci 32: 1975–1982.
30. Ohta H, Sato K, Murata N, Damirin A, Malchinkhuu E, et al. (2003) Ki16425, a subtype-selective antagonist for EDG-family lysophosphatidic acid receptors. Mol Pharmacol 64: 994–1005.
31. Ma L, Matsumoto M, Xie W, Inoue M, Ueda H (2009) Evidence for lysophosphatidic acid 1 receptor signaling in the early phase of neuropathic pain mechanisms in experiments using Ki-16425, a lysophosphatidic acid 1 receptor antagonist. J Neurochem 109: 603–610.
32. Shindou H, Hishikawa D, Nakanishi H, Harayama T, Ishii S, et al. (2007) A single enzyme catalyzes both platelet-activating factor production and membrane biogenesis of inflammatory cells. Cloning and characterization of acetyl-CoA:LYSO-PAF acetyltransferase. J Biol Chem 282: 6532–6539.

33. Harayama T, Shindou H, Ogasawara R, Suwabe A, Shimizu T (2008) Identification of a novel noninflammatory biosynthetic pathway of platelet-activating factor. J Biol Chem 283: 11097–11106.
34. Kihara Y, Yanagida K, Masago K, Kita Y, Hishikawa D, et al. (2008) Platelet-activating factor production in the spinal cord of experimental allergic encephalomyelitis mice via the group IVA cytosolic phospholipase A2-lyso-PAFAT axis. J Immunol 181: 5008–5014.
35. Ishii S, Shimizu T (2000) Platelet-activating factor (PAF) receptor and genetically engineered PAF receptor mutant mice. Prog Lipid Res 39: 41–82.
36. Ishii S, Kuwaki T, Nagase T, Maki K, Tashiro F, et al. (1998) Impaired anaphylactic responses with intact sensitivity to endotoxin in mice lacking a platelet-activating factor receptor. J Exp Med 187: 1779–1788.
37. Tsuda M, Ishii S, Masuda T, Hasegawa S, Nakamura K, et al. (2007) Reduced pain behaviors and extracellular signal-related protein kinase activation in primary sensory neurons by peripheral tissue injury in mice lacking platelet-activating factor receptor. J Neurochem 102: 1658–1668.
38. Schafers M, Geis C, Svensson CI, Luo ZD, Sommer C (2003) Selective increase of tumour necrosis factor-alpha in injured and spared myelinated primary afferents after chronic constrictive injury of rat sciatic nerve. Eur J Neurosci 17: 791–804.
39. Kihara Y, Ishii S, Kita Y, Toda A, Shimada A, et al. (2005) Dual phase regulation of experimental allergic encephalomyelitis by platelet-activating factor. J Exp Med 202: 853–863.
40. Fernandes ES, Passos GF, Campos MM, de Souza GE, Fittipaldi JF, et al. (2005) Cytokines and neutrophils as important mediators of platelet-activating factor-induced kinin B1 receptor expression. Br J Pharmacol 146: 209–216.
41. Hefferan MP, O'Rielly DD, Loomis CW (2003) Inhibition of spinal prostaglandin synthesis early after L5/L6 nerve ligation prevents the development of prostaglandin-dependent and prostaglandin-independent allodynia in the rat. Anesthesiology 99: 1180–1188.
42. Zhu X, Eisenach JC (2003) Cyclooxygenase-1 in the spinal cord is altered after peripheral nerve injury. Anesthesiology 99: 1175–1179.
43. Zhao Z, Chen SR, Eisenach JC, Busija DW, Pan HL (2000) Spinal cyclooxygenase-2 is involved in development of allodynia after nerve injury in rats. Neuroscience 97: 743–748.
44. Kost RG, Straus SE (1996) Postherpetic neuralgia–pathogenesis, treatment, and prevention. N Engl J Med 335: 32–42.
45. Samuelsson B (1983) Leukotrienes: mediators of immediate hypersensitivity reactions and inflammation. Science 220: 568–575.
46. Levine JD, Lau W, Kwiat G, Goetzl EJ (1984) Leukotriene B4 produces hyperalgesia that is dependent on polymorphonuclear leukocytes. Science 225: 743–745.
47. Levine JD, Lam D, Taiwo YO, Donatoni P, Goetzl EJ (1986) Hyperalgesic properties of 15-lipoxygenase products of arachidonic acid. Proc Natl Acad Sci U S A 83: 5331–5334.
48. Doi K, Okamoto K, Negishi K, Suzuki Y, Nakao A, et al. (2006) Attenuation of folic acid-induced renal inflammatory injury in platelet-activating factor receptor-deficient mice. Am J Pathol 168: 1413–1424.
49. Scholz J, Woolf CJ (2007) The neuropathic pain triad: neurons, immune cells and glia. Nat Neurosci 10: 1361–1368.
50. Marchand F, Perretti M, McMahon SB (2005) Role of the immune system in chronic pain. Nat Rev Neurosci 6: 521–532.
51. Mantyh PW (2006) Cancer pain and its impact on diagnosis, survival and quality of life. Nat Rev Neurosci 7: 797–809.
52. Moalem G, Tracey DJ (2006) Immune and inflammatory mechanisms in neuropathic pain. Brain Res Rev 51: 240–264.
53. Schafers M, Geis C, Brors D, Yaksh TL, Sommer C (2002) Anterograde transport of tumor necrosis factor-alpha in the intact and injured rat sciatic nerve. J Neurosci 22: 536–545.
54. Li H, Xie W, Strong JA, Zhang JM (2007) Systemic antiinflammatory corticosteroid reduces mechanical pain behavior, sympathetic sprouting, and elevation of proinflammatory cytokines in a rat model of neuropathic pain. Anesthesiology 107: 469–477.
55. Uceyler N, Tscharke A, Sommer C (2007) Early cytokine expression in mouse sciatic nerve after chronic constriction nerve injury depends on calpain. Brain Behav Immun 21: 553–560.
56. Sacerdote P, Franchi S, Trovato AE, Valsecchi AE, Panerai AE, et al. (2008) Transient early expression of TNF-alpha in sciatic nerve and dorsal root ganglia in a mouse model of painful peripheral neuropathy. Neurosci Lett 436: 210–213.
57. Jin X, Gereau RWt (2006) Acute p38-mediated modulation of tetrodotoxin-resistant sodium channels in mouse sensory neurons by tumor necrosis factor-alpha. J Neurosci 26: 246–255.
58. Liu L, Yang TM, Liedtke W, Simon SA (2006) Chronic IL-1beta signaling potentiates voltage-dependent sodium currents in trigeminal nociceptive neurons. J Neurophysiol 95: 1478–1490.
59. Elmes SJ, Millns PJ, Smart D, Kendall DA, Chapman V (2004) Evidence for biological effects of exogenous LPA on rat primary afferent and spinal cord neurons. Brain Res 1022: 205–213.
60. Renback K, Inoue M, Ueda H (1999) Lysophosphatidic acid-induced, pertussis toxin-sensitive nociception through a substance P release from peripheral nerve endings in mice. Neurosci Lett 270: 59–61.
61. Hasegawa S, Kohro Y, Tsuda M, Inoue K (2009) Activation of cytosolic phospholipase A2 in dorsal root ganglion neurons by Ca2+/calmodulin-dependent protein kinase II after peripheral nerve injury. Mol Pain 5: 22.
62. Lindsberg PJ, Hallenbeck JM, Feuerstein G (1991) Platelet-activating factor in stroke and brain injury. Ann Neurol 30: 117–129.
63. Kim SH, Chung JM (1992) An experimental model for peripheral neuropathy produced by segmental spinal nerve ligation in the rat. Pain 50: 355–363.
64. Tsuda M, Shigemoto-Mogami Y, Koizumi S, Mizokoshi A, Kohsaka S, et al. (2003) P2X4 receptors induced in spinal microglia gate tactile allodynia after nerve injury. Nature 424: 778–783.
65. Tsuda M, Masuda T, Kitano J, Shimoyama H, Tozaki-Saitoh H, et al. (2009) IFN-gamma receptor signaling mediates spinal microglia activation driving neuropathic pain. Proc Natl Acad Sci U S A 106: 8032–8037.
66. Obata K, Yamanaka H, Kobayashi K, Dai Y, Mizushima T, et al. (2004) Role of mitogen-activated protein kinase activation in injured and intact primary afferent neurons for mechanical and heat hypersensitivity after spinal nerve ligation. J Neurosci 24: 10211–10222.

Journal of Neurochemistry JNC

JOURNAL OF NEUROCHEMISTRY | 2010 | 114 | 810–819 doi: 10.1111/j.1471-4159.2010.06809.x

P2X7 receptor activation induces CXCL2 production in microglia through NFAT and PKC/MAPK pathways

Miho Shiratori,[1] Hidetoshi Tozaki-Saitoh,[1] Mai Yoshitake, Makoto Tsuda and Kazuhide Inoue

Department of Molecular and System Pharmacology, Graduate School of Pharmaceutical Sciences, Kyushu University, Fukuoka, Japan

Abstract

Microglia plays an important role in many neurodegenerative conditions. ATP leaked or released by damaged cells triggers microglial activation through P2 receptors, and stimulates the release of oxygen radicals, proinflammatory cytokines and chemokines from activated microglia. However, little is known about mechanisms underlying ATP-induced chemokine release from microglia. In this study, we found that a high concentration of ATP induces the mRNA expression and release of CXCL2 from microglia. A similar effect was observed following treatment of microglia with a P2X7 receptor (P2X7R) agonist, 2′-and 3′-*O*-(4-benzoylbenzoyl) ATP, and this was inhibited by pre-treatment with a P2X7R antagonist, Brilliant Blue G. ATP induced both activation of nuclear factor of activated T cells (NFAT) and MAPKs (p38, ERK, and JNK) through P2X7R. ATP-induced mRNA expression of CXCL2 was inhibited by INCA-6 (an NFAT inhibitor), SB203580 (a p38 inhibitor), U0126 (a MEK-ERK inhibitor) and JNK inhibitor II (a JNK inhibitor). However, MAPK inhibitors did not inhibit activation of NFAT. In addition, protein kinase C inhibitors suppressed ATP-induced ERK and JNK activation, and also inhibited ATP-induced CXCL2 expression in microglia. These results suggest that ATP increased CXCL2 production via both NFAT and protein kinase C/MAPK signaling pathways through P2X7 receptor stimulation in microglia.

Keywords: ATP, chemokine, CXCL2, microglia, P2X7, release.

J. Neurochem. (2010) **114**, 810–819.

Microglia, one of the types of glial cells in the CNS, plays an important role as resident immunocompetent and phagocytic cells during infection, inflammation, trauma, ischemia, and other neurodegenerative conditions. ATP leaked or released by damaged cells as a result of many neurodegenerative conditions triggers microglial activation through P2 receptors (Inoue 2002). Activated microglia release substances such as oxygen radicals (Parvathenani *et al.* 2003), proinflammatory cytokines (Ferrari *et al.* 1997b; Hide *et al.* 2000; Shigemoto-Mogami *et al.* 2001), and chemokines (Kataoka *et al.* 2009).

Microglia have been shown to express multiple P2 receptor subtypes, including P2X4, P2X7, P2Y2, P2Y6, and P2Y12 (Norenberg *et al.* 1994; James and Butt 2002; Tsuda *et al.* 2003; Koizumi *et al.* 2007). Among them, the P2X7 receptor (P2X7R) is a non-selective cation channel, and requires a high concentration (millimolar levels) of ATP for its activation (Steinberg *et al.* 1987; Greenberg *et al.* 1988). It is widely acknowledged that P2X7R is involved in various CNS pathologies including ischemia (Le Feuvre *et al.* 2003; Franke *et al.* 2004), Alzheimer's disease (Parvathenani *et al.* 2003; McLarnon *et al.* 2006), multiple sclerosis (Yiangou *et al.* 2006), and neuropathic pain (Chessell *et al.* 2005; Honore *et al.* 2006), by regulating the expression and release of cytokines and inflammatory mediators.

Following activation of P2X7R by ATP, multiple transcriptional factors responsible for inflammatory gene expression can be activated (Ferrari *et al.* 1997a, 1999; Potucek *et al.* 2006). Nuclear factor of activated T cells (NFAT) is also known to control the expression of many inflammatory

Received March 4, 2010; revised manuscript received April 19, 2010; accepted May 4, 2010.

Address correspondence and reprint requests to Kazuhide Inoue, Department of Molecular and System Pharmacology, Graduate School of Pharmaceutical Sciences, Kyushu University, 3-1-1 Maidashi, Higashi, Fukuoka 812-8582, Japan. E-mail: inoue@phar.kyushu-u.ac.jp

[1]These authors contributed equally to this study.

Abbreviations used: AP-1, activator protein 1; AREs, AU-rich elements; BBG, Brilliant Blue G; BzATP, 2′-and 3′-*O*-(4-benzoylbenzoyl) ATP; ERK, extracellular signal-regulated Kinase; INCA-6, inhibitor of NFAT-calcineurin association-6; JNK, c-Jun N-terminal kinase; MIP, macrophage inflammatory protein; NFAT, nuclear factor of activated T cells; NF-κB, nuclear factor-κB; P2X7R, P2X7 receptor; PBS, phosphate-buffered saline; PKC, protein kinase C.

genes including IL-1β, interferon-γ, Granulocyte Macrophage colony-stimulating Factor, IL-2, and CCL3. Dephosphorylation of NFAT by calcineurin, a calcium-dependent phosphatase, exposes a nuclear localization sequence in the NFAT protein, permitting nuclear translocation and subsequent transcriptional activation (Rao *et al.* 1997; Im and Rao 2004; Kataoka *et al.* 2009).

MAPK pathways are also known to be activated by ATP and integral to the regulation of inflammatory gene expression (Potucek *et al.* 2006). It is reported that both extracellular signal-regulated Kinase (ERK) and c-Jun N-terminal kinase (JNK) are involved in the regulation of ATP-induced tumor necrosis factor-α mRNA expression in microglia (Suzuki *et al.* 2004).

CXCL2 belongs to the CXC chemokine family, and interacts with the chemokine receptor CXCR2 (Pelus and Fukuda 2006). CXCL2 has potent chemotactic activity for neutrophils (Tessier *et al.* 1997). We previously found that ATP induces production of a CC chemokine, CCL3 in microglia (Kataoka *et al.* 2009). CCL3 and CXCL2 commonly induce neutrophil infiltration, followed by aggravation of inflammation or tissue damage. In bacterial meningitis, both chemokines are simultaneously up-regulated, and anti-macrophage inflammatory protein (MIP)-1α or anti-MIP-2 antibodies significantly reduced neutrophil infiltration (Diab *et al.* 1999). In this way, CCL3 and CXCL2 play a central role in pathologies inducing neutrophil infiltration. Moreover, previous reports indicate that CXCR2 is involved in Alzheimer's disease (Bakshi *et al.* 2009), ischemia (Popivanova *et al.* 2003), traumatic injury (Valles *et al.* 2006), multiple sclerosis (Kerstetter *et al.* 2009), neuronal death (De Paola *et al.* 2007) and opioid receptor function (Parenty *et al.* 2008). However, although the importance of CXCR2 in various CNS pathologies has been reported, little is known about a source of ligands for CXCR2 including CXCL2.

In the present study, we show that ATP induces mRNA expression and release of CXCL2 mainly through activation of P2X7R in microglia and that calcineurin-dependent NFAT activation and protein kinase C (PKC)/MAPK pathways downstream of P2X7R are implicated in the mRNA expression of CXCL2.

Materials and methods

Cell culture

The mouse microglial cell line, BV-2 (kindly provided by Dr. Biber K., Department of Medical Physiology, University Medical Center Groningen, University of Groningen) were cultured in Dulbecco's modified Eagle's medium with 5% heat- inactivated fetal bovine serum, 2 mM L-Glutamine, penicillin and streptomycin.

Rat primary cultured microglia was prepared according to the method described previously (Nakajima *et al.* 1992; Tsuda *et al.* 2003). In brief, the mixed glial culture was prepared from neonatal Wister rats and maintained for 9–15 days in Dulbecco's modified Eagle's medium with 10% fetal bovine serum. Microglia obtained as floating cells were collected by gentle shaking and transferred to appropriate culture plate.

Quantitative RT-PCR analysis

BV-2 cells were plated onto 24 well plates ($0.8–1 \times 10^5$ cells/well) and incubated at 37°C for 24 h. Then the BV-2 cells were washed with serum-free medium and further incubated with the fresh serum-free medium for 12 h. Rat primary cultured microglia were cultured 24 well plates ($2–4 \times 10^5$ cells/well) for 1 h, and then cells were incubated for 1 h with serum-free medium. After incubation, the cells were stimulated with agonists and later the cells were lysed in TRIsure (Bioline, London, UK) including glycogen and total RNA was extracted. RT-PCR was performed using the Takara One Step Prime Script RT-PCR kit according to manufacturer's protocol. Data were obtained using an ABI Prism 7500 sequence detection system (Applied Biosystems, Foster City, CA, USA) and analyzed using 7500 System SDS Software 1.3.1 (Applied Biosystems). The CXCL2 mRNA expression levels were normalized to the levels of 18S ribosomal RNA. The sequences of the forward and reverse primers for mouse CXCL2 were 5′-CGCTGTCAATGCCTGAAGAC-3′ and 5′-CCTTGAGAGTGGCTATGACTTCTG-3′, and for rat CXCL2 were 5′-ACAACAACCCCTGTACCCTGAT-3′ and 5′-GCCAGCTCC TCAATGCTGTACT-3′, respectively. The TaqMan fluorogenic probe was FAM-TCCAGAGCTTGAGTGTGACGCCCC-TAMRA-3′.

Measurement of CXCL2 release

BV-2 cells and rat primary cultured microglia were plated onto 24 well plates as same as quantitative RT-PCR. After pre-treatment with antagonists or inhibitors for 10 min, the cells were stimulated with agonists. At appropriate time after stimulation, supernatants were collected. The concentrations of CXCL2 in each sample were determined by mouse MIP-2 ELISA Kits (R&D Systems, Minneapolis, MN, USA) and rat CXCL2/CINC-3 Quantikine ELISA Kits (R&D Systems). The assay was performed according to manufacturer's protocol.

Immunocytochemistry

BV-2 cells were seeded on poly-L-lysin coated glass ($1–1.5 \times 10^4$ cells/well) and incubated for the same schedule as quantitative RT-PCR. After pre-treatment with antagonists or inhibitors for 10 min, the cells were stimulated with agonists for 30 min and then fixed in 3.7% formaldehyde in phosphate-buffered saline (PBS) for 30 min. The cells were incubated for 15 min in blocking solution: PBS with 3% normal goat serum and 0.3% Triton X-100, and then incubated overnight at 4°C with primary antibodies [NFATc2 (1 : 1000) and Iba1 (1 : 1000)]. After overnight incubation, the cells were washed and incubated for 1 h with secondary antibodies [Anti-mouse IgG-conjugated Alexa 488 and Anti-rabbit IgG-conjugated Alexa 546 (1 : 1000)] and mounted in VECTASHIELD with DAPI (Vector Laboratories, Burlingame, CA, USA). The observations were performed under a confocal microscope (LSM510, Carl Zeiss Japan, Tokyo, Japan).

Western blot analysis

BV-2 cells were plated onto 24 well plates as same as quantitative RT-PCR. After pre-treatment with antagonists or inhibitors for 10 min, the cells were stimulated with agonists. At appropriate time

after stimulation, the cells were lysed for 30 min on ice in cell extraction buffer. The detergent-insoluble material was removed by centrifugation at 21 600 *g* for 10 min at 4°C. Samples were resuspended in sodium dodecyl sulfate–polyacrylamide gel electrophoresis loading buffer, boiled for 5 min, and analyzed by 10% sodium dodecyl sulfate–polyacrylamide gel electrophoresis. The resolved proteins were transferred onto polyvinylidene difluoride membranes. Then membranes were blocked for 1 h in Tris-buffered saline with 0.1% Tween 20 and 5% bovine serum albumin. After incubations with first and second Abs and washing with PBS with 0.1% Tween 20, visualization of specific proteins was conducted using ECL western blotting detection regents (GE Healthcare Japan, Tokyo, Japan) and analyzed using an LAS-3000 imaging system (Fuji Photo Film Co., Ltd, Tokyo, Japan).

Reagents and antibodies

ATP, ADP, UTP, UDP, 2′-and 3′-*O*-(4-benzoylbenzoyl) ATP (BzATP), suramin, 4-([4-formyl-5-hydroxy-6-methyl-3-[(phosphonooxy)methyl]-2-pyridinyl]azo]-1,3-benzenedisulfonic acid (PPADS), bovine serum albumin, Brilliant Blue G (BBG) and anti-β-actin mouse monoclonal antibody were from Sigma Chemical Co. (St Louis, MO, USA). Cyclosporin A was from Biomol International LP (PE, USA). Gö 6983, Bisindolylmaleimide I (Bis), and the NFAT inhibitor 'inhibitor of NFAT-calcineurin association-6' (INCA-6) were from EMD Biosciences, Inc. (San Diego, CA, USA). EDTA was from Wako (Tokyo, Japan). Antibody against NFATc2 (25A10) was from Thermo Fisher Scientific Inc. (Rockford, IL, USA). Antibodies against ERK, JNK, p38 were from Cell Signaling Technology Japan (Tokyo, Japan). U0126 was from Promega. JNK inhibitor II (SP600125) was from Cayman Chemical (Ann Arbor, MI, USA). SB203580 was from Tocris Bioscience (Bristol, UK).

Data analysis and statistics

All results are expressed as the mean ± SEM. A statistical analysis was performed using one-way ANOVA or two-way ANOVA followed by Tukey's multiple comparison tests. Statistically significant differences from controls are indicated by $***p < 0.001$ and $*p < 0.05$. Statistically significant differences from ATP treated samples are indicated by $\#\#\#p < 0.001$, $\#\#p < 0.01$ and $\#p < 0.05$.

Results

ATP induces release and mRNA expression of CXCL2 in microglia

Extracellular ATP can induce release and expression of proinflammatory cytokines in microglia. We first confirmed that 1 mM ATP induced CXCL2 release in BV-2 cells (Fig. 1a–c), an immortalized mouse microglial cell line (Blasi *et al.* 1990). This release was observed only in the presence of high concentrations of ATP (1000 μM)

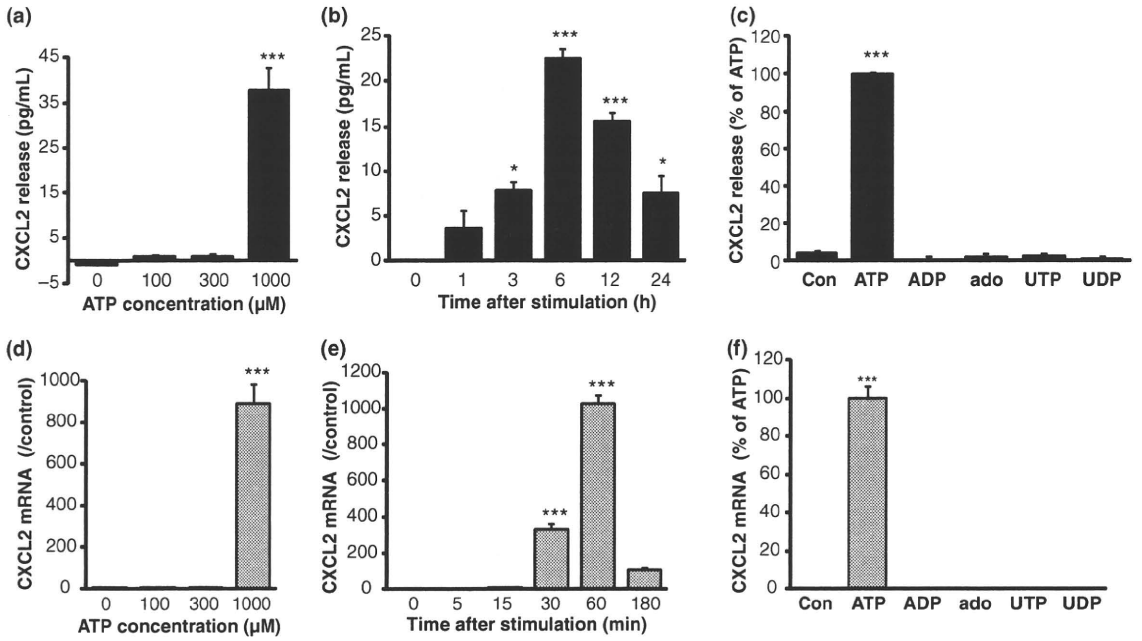

Fig. 1 ATP induces CXCL2 release and expression in microglia. (a and d) Dose-dependent release and expression of CXCL2. BV-2 microglial cells were incubated with various concentration of ATP for 6 h (release; a) and 1 h (expression; d). (b and e) The time course of release and expression of CXCL2. BV-2 microglial cells were incubated with 1 mM ATP for 1, 3, 6, 9, 12, or 24 h (release; b) and for 15, 30, 60, and 180 min (expression; e). (c and f) Effects of various nucleotides on CXCL2 release and expression. BV-2 microglial cells were incubated with ATP (1 mM), ADP (50 μM), adenosine (100 μM), UTP (100 μM), and UDP (100 μM) for 6 h (release; c), and for 1 h (expression; f). The supernatant were collected to measure release of CXCL2, and total RNA was extracted and subjected to real-time RT-PCR for CXCL2. CXCL2 expression values are shown as the ratio to 18S ribosomal RNA. Results are expressed as the mean ± SEM in triplicate. At least two independent experiments performed and similar results were obtained. *, $p < 0.05$ compared with 0 h; ***, $p < 0.001$ compared with 0 (μM, h or min) or control.

(Fig. 1a), and peaked at 6 h after ATP treatment, lasting for at least 24 h in BV-2 cells (Fig. 1b). To investigate whether the ATP-induced release of CXCL2 is correlated with transcriptional activity, we performed quantitative RT-PCR analysis. The level of the mRNA for CXCL2 was significantly increased at 30 min after 1 mM ATP treatment, and peaked at 1 h after ATP treatment (Fig. 1e). This increase was also observed only in the presence of high concentrations of ATP (1000 μM) (Fig. 1d). Nucleotides other than ATP could not induce release and mRNA expression of CXCL2 (Fig. 1c and f). To enforce our idea and confirm that mechanisms described here were not just mechanisms only in a specific cell line, we used primary microglia and found that CXCL2 release was induced in both mouse and rat primary microglia by ATP stimulation (Figure S1c and g).

Involvement of P2X7 receptor in ATP-induced CXCL2 production

Among several P2 receptors expressed on microglia, we focused on the P2X7 receptor (P2X7R) because high concentrations of ATP were required for release and mRNA expression of CXCL2 (Fig. 1a and d), and nucleotides other than ATP that activate P2Y receptors did not induce release and mRNA expression of CXCL2 (Fig. 1c and f). We investigated whether P2X7Rs are involved in ATP-induced release and mRNA expression of CXCL2 in microglia using an agonist and antagonists of P2X7R. The potent P2X7R agonist, BzATP (300 μM) induced release and mRNA expression of CXCL2 in BV-2 cells (Fig. 2a and c). Pre-treatment of the cells with suramin (1 mM) or 4-([4-formyl-5-hydroxy-6-methyl-3-[(phosphonooxy)methyl]-2-pyridinyl] azo]-1,3-benzenedisulfonic acid (100 μM), which are broad spectrum-antagonists for P2 receptors, or the selective antagonist of P2X7R BBG (1 μM) significantly inhibited ATP-induced release and mRNA expression of CXCL2 in BV-2 cells (Fig. 2d and b). BBG also showed significant inhibition in ATP-induced CXCL2 release from primary microglia (Figure S1c and g), but the rate of inhibition are smaller than that of observed in BV-2 cell (Figs 2b and S1c,g). Furthermore, because P2X7R is well-known as a non-selective cation channel, we investigated the involvement of extracellular Ca^{2+} influx in ATP-induced mRNA expression of CXCL2 using the extracellular Ca^{2+} chelator EDTA (2 mM). Treatment with EDTA significantly inhibited ATP-induced mRNA expression of CXCL2 in BV-2 cells (Fig. 2d). These data indicate that Ca^{2+} influx via activation of P2X7R is involved in ATP-induced release and mRNA expression of CXCL2.

Involvement of calcineurin-dependent NFAT activation in ATP-induced mRNA expression of CXCL2

It has been reported that NFAT proteins play an important role in the transcription of several inducible cytokines such as IL-2, IL-4, interferon, Granulocyte Macrophage colony-

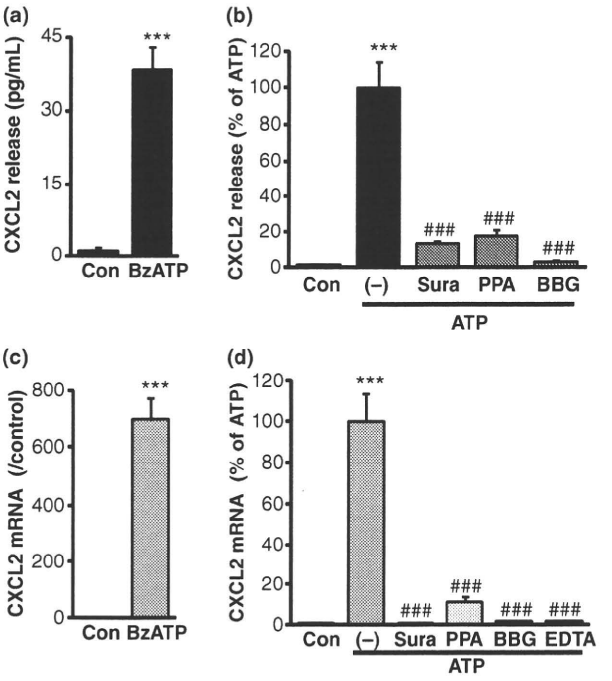

Fig. 2 P2X7R is involved in ATP-induced CXCL2 expression. Effects of the potent P2X7R agonist, BzATP (300 μM) on CXCL2 expression (c) and release (a) in BV-2 cells. Pre-treatment for 10 min with suramin (sura, 1 mM), PPADS (PPA, 100 μM), and the selective antagonist of P2X7R, BBG (1 μM) significantly inhibited ATP-induced CXCL2 expression (d) and release (b), and EDTA also inhibited ATP-induced CXCL2 expression in BV-2 cells (d). Cells were treated with ATP for 6 h (release) and 1 h (expression), and co-treated with ATP and EDTA (2 mM) for 1 h. All inhibitors and antagonists did not show cytotoxicity. Results of BV-2 cells are expressed as the mean ± SEM in triplicate. At least two independent experiments performed and similar results were obtained. ***, $p < 0.001$ compared with control; ###, $p < 0.001$ compared with ATP.

stimulating Factor, and tumor necrosis factor (Rao 1994; Rao *et al.* 1997; Im and Rao 2004). ATP-induced NFAT activation requires extracellular Ca^{2+} influx, mainly through P2X7R (Ferrari *et al.* 1999), and occurs in parallel with nuclear localization of NFAT protein (Kataoka *et al.* 2009). In BV-2 cells, ATP (1 mM) and BzATP (300 μM) induced nuclear localization of NFAT (Fig. 3a). Induction of NFAT transcriptional activity by ATP stimulation was confirmed by luciferase reporter assay of NFAT response element (Figure S2). Furthermore, pre-treatment of these cells with BBG (1 μM) prevented ATP-induced nuclear localization of NFAT (Fig. 3a). These results suggested that ATP induces NFAT activation through P2X7R in BV-2 cells. Next, to investigate the involvement of NFAT activation in ATP-induced CXCL2 expression, we used the calcineurin inhibitor cyclosporine A (CsA, 10 ng/mL) and the NFAT-selective inhibitor INCA-6 (10 μM) (Roehrl *et al.* 2004). Pre-treatment of BV-2 cells with cyclosporine A and INCA-6 significantly inhibited ATP-induced CXCL2

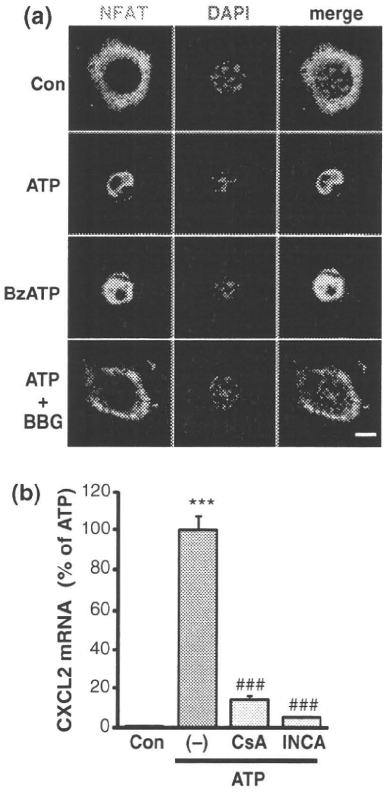

Fig. 3 Calcineurin-dependent NFAT activation through P2X7R is involved in ATP-induced CXCL2 expression. (a) Nuclear translocation of NFATc2 (green) at 30 min after ATP (1 mM) stimulation, and effects of BBG (1 μM) on ATP-induced nuclear translocation of NFATc2. BV-2 microglial cells were pre-treated with BBG for 10 min before ATP treatment. After treatment, cells were fixed and stained using anti-NFATc2 Ab. At least two independent experiments were performed and similar results were obtained. Scale bar, 10 μm. (b) Effects of calcineurin inhibitor, CsA (10 ng/μL) and NFAT inhibitor, INCA-6 (INCA, 10 μM) on ATP-induced CXCL2 expression. BV-2 microglial cells were pre-treated with CsA and INCA-6 for 10 min before ATP treatment. ATP treatment was for 1 h. Results are expressed as the mean ± SEM in triplicate. At least two independent experiments performed and similar results were obtained. Cells were pre-treated with CsA or INCA-6 for 10 min before ATP treatment. ATP treatment was for 1 h. Results are expressed as the mean ± SEM in triplicate of two independent experiments. ***, $p < 0.001$ compared with control; ###, $p < 0.001$ compared with ATP.

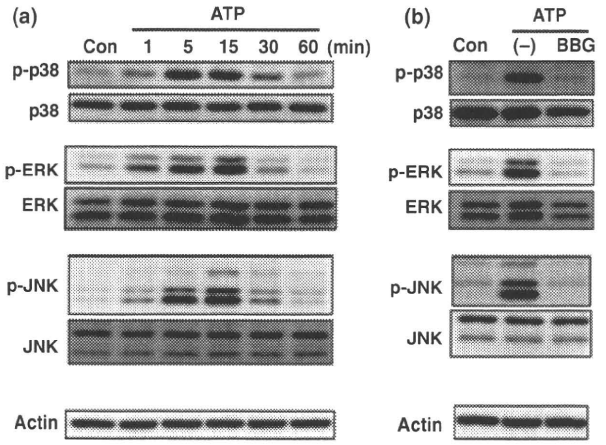

Fig. 4 ATP-induced p38, MEK/ERK and JNK activation require P2X7R activation. (a) Time-course of phosphorylation of p38, ERK, and JNK. BV-2 microglial cells were incubated with ATP (1 mM) for indicated time intervals, and phosphorylation of each MAPK was determined by immunoblotting using phospho-each MAPK-specific Ab. (b) Effects of BBG (1 μM) on ATP-induced p38, ERK, and JNK phosphorylation. BV-2 microglial cells were pre-treated with BBG for 10 min before ATP treatment. ATP treatment was for 15 min. At least two independent experiments were performed and similar results were obtained.

expression in BV-2 cells (Fig. 3b). INCA-6 also inhibited ATP-induced CXCL2 expression in rat primary microglia (Figure S1d). These data suggested that calcineurin-dependent NFAT activation through P2X7R is required for ATP-induced mRNA expression of CXCL2.

P38, MEK/ERK and JNK signaling pathways are involved in ATP-induced mRNA expression of CXCL2

In macrophages and monocytes, P2X7R stimulation rapidly activates p38, ERK (Aga *et al.* 2002), and JNK (Humphreys *et al.* 2000). In microglia, it is suggested that activation of P2X7R is potent in activating these kinases (Potucek *et al.* 2006). We found that ATP (1 mM) induced phosphorylation of p38, ERK and JNK in BV-2 cells (Fig. 4a). Pre-treatment of cells with BBG (1 μM) prevented ATP-induced phosphorylation of these molecules (Fig. 4b). These data suggested that ATP induces activation of p38, ERK and JNK through P2X7R. Next, we investigated whether these MAPKs are involved in ATP-induced mRNA expression of CXCL2 using MAPK inhibitors. Pre-treatment of BV-2 cells with the p38 inhibitor SB203580, the MAPK/ERK kinase (MEK)/ERK inhibitor U0126 and the JNK inhibitor JNK inhibitor II (SP600125) inhibited ATP-induced mRNA expression of CXCL2 (Fig. 5a). SB203580 and U0126 also inhibited ATP-induced CXCL2 expression in rat primary microglia. SB203580 inhibited even control expression of CXCL2. We could not investigate the effect of JNK inhibitor because of its cytotoxicity (Figure S1e). These results suggest that activation of p38, MEK/ERK and JNK via activation of P2X7R is involved in ATP-induced mRNA expression of CXCL2 in microglia.

Activation of MAPKs does not regulate ATP-induced nuclear localization of NFAT

The results of this study suggested that NFAT and MAPKs are involved in ATP-induced CXCL2 expression. Because pre-treatment of cells with NFAT and MAPK inhibitors markedly inhibited ATP-induced CXCL2 expression, it is

